Double-Decker Actinide Porphyrins and Phthalocyanines. Synthesis and Spectroscopic Characterization of Neutral, Oxidized, and Reduced Homo- and Heteroleptic Complexes

K. M. Kadish,*,† G. Moninot,† Y. Hu,† D. Dubois,† A. Ibnlfassi,‡ J.-M. Barbe,‡ and R. Guilard*,‡

Contribution from the Department of Chemistry, University of Houston, Houston, Texas 77204-5641, and Laboratoire de Synthèse et d'Electrosynthèse Organométalliques associé au C.N.R.S., U.R.A. 33, Faculté des Sciences "Gabriel", 6, Bd Gabriel, 21100 Dijon, France

Received December 22, 1992. Revised Manuscript Received May 10, 1993

Abstract: The synthesis, spectroscopic characterization, and electrochemistry of 26 different neutral and singly-oxidized homoleptic and heteroleptic actinide double-decker complexes are reported. The investigated compounds are represented as $[M(P)_2]^n$, $[M(P)(P')]^n$, $[M(Pc)_2]^n$, and $[M(P)(Pc)]^n$ where n = 0 or 1+, M = U or Th, Pc = the dianion of phthalocyanine, and P or P′ = the dianions of octaethylporphyrin (OEP), tetraphenylporphyrin (TPP), or tetra-*p*-tolylporphyrin (TpTP). Each neutral compound was characterized by ^{1}H NMR, UV-visible, and IR spectroscopy and comparisons made to the cationic singly-oxidized double-decker derivatives which were chemically generated and isolated as a $SbCl_6^-$ salt. The initial neutral species can undergo up to six reversible one-electron transfers in nonaqueous media, and U(IV) or Th(IV) compounds with a given set of porphyrin or phthalocyanine macrocycles could be electrogenerated in up to seven different oxidation states. Some of these species were characterized by UV-visible or FTIR thin-layer spectroelectrochemistry and the resulting spectral data then used along with the redox potentials to assign the site of each electron transfer. The first two reductions of M(P)(Pc) occur mainly at the Pc ring while the first two oxidations of the same heteroleptic compound involve primarily orbitals of the porphyrin macrocycle. This result contrasts with the homoleptic $M(P)_2$ and $M(Pc)_2$ derivatives which undergo initial one-electron oxidations and reductions which are localized not at a single porphyrin or phthalocyanine ring but rather at orbitals involving both macrocycles. The ESR spectra of $[Th(OEP)(Pc)]^+$ and $[Th(TPP)(Pc)]^+$ show triplet character in toluene or methylene chloride and give data consistent with the presence of dimers held together by π–π interactions between two Pc macrocycles. The calculated distance between the two electrons in the dimer varies between 8.8 and 9.0 Å, which is consistent with the hole of $[Th(P)(Pc)]^+$ being localized on the porphyrin ring and the two cation radicals being separated in the π–π complex by an average of about 3.3 Å. No π–π interactions are observed for the singly-oxidized homoleptic species, and the ESR spectra of $[Th(P)_2]^+$ and $[Th(Pc)_2]^+$ suggest simple monomeric cation radicals, both as $SbCl_6^-$ salts in the solid state and in frozen solutions of CH_2Cl_2 or pyridine at 110 K.

Introduction

Lanthanide and actinide porphyrin sandwich complexes of the type $[M^{III}(P)_2]^-$, $M^{IV}(P)_2$, and $M^{III}_2(P)_3$ have provided an ideal series of molecules for studying the electronic structure and dynamics of interacting porphyrin macrocycles.[1-27] These double-[1-24] and triple-decker[1-5,25-27] complexes have been synthesized mainly with identical, symmetrical macrocycles, but complexes with dissimilar, asymmetrical macrocycles are also known and have been studied in large part for derivatives of Ce(IV),[19-21,28,29] Th(IV),[22] Eu(III),[14,30] or La(III).[24]

† University of Houston.
‡ Faculté des Sciences "Gabriel".

(1) Buchler, J. W.; De Cian, A.; Fischer, J.; Kihn-Botulinski, M.; Paulus, H.; Weiss, R. *J. Am. Chem. Soc.* **1986**, *108*, 3652–3659.
(2) Buchler, J. W.; Scharbert, B. *J. Am. Chem. Soc.* **1988**, *110*, 4272–4276.
(3) Buchler, J. W.; De Cian, A.; Fischer, J.; Kihn-Botulinski, M.; Weiss, R. *Inorg. Chem.* **1988**, *27*, 339–345.
(4) Buchler, J. W.; Kapellmann, H. G.; Knoff, M.; Lay, K.-L.; Pfeifer, S. *Z. Naturforsch.* **1983**, *38b*, 1339–1345.
(5) Buchler, J. W.; Elsässer, K.; Kihn-Botulinski, M.; Scharbert, B. *Angew. Chem., Int. Ed. Engl.* **1986**, *25*, 286–287.
(6) Duchowski, J. K.; Bocian, D. F. *J. Am. Chem. Soc.* **1990**, *112*, 3312–3318.
(7) Yau, X.; Holten, D. *J. Phys. Chem.* **1988**, *92*, 409–414.
(8) Bilsel, O.; Rodriguez, J.; Holten, D.; Girolami, G. S.; Milam, S. N.; Suslick, K. S. *J. Am. Chem. Soc.* **1990**, *112*, 4075–4077.
(9) Girolami, G. S.; Milam, S. N.; Suslick, K. S. *Inorg. Chem.* **1987**, *26*, 343–344.
(10) Buchler, J. W.; Hammerschmitt, P.; Kaufeld, I.; Löffler, J. *Chem. Ber.* **1991**, *124*, 2151–2159.
(11) Buchler, J. W.; De Cian, A.; Fischer, J.; Hammerschmitt, P.; Weiss, R. *Chem. Ber.* **1991**, *124*, 1051–1058.
(12) Buchler, J. W.; Hüttermann, J.; Löffler, J. *Bull. Chem. Soc. Jpn.* **1988**, *61*, 71–77.
(13) Buchler, J. W.; Kihn-Botulinski, M.; Scharbert, B. *Z. Naturforsch.* **1988**, *43b*, 1371–1380.
(14) Buchler, J. W.; Löffler, J. *Z. Naturforsch.* **1990**, *45b*, 531–542.
(15) Donohoe, R. J.; Duchowski, J. K.; Bocian, D. F. *J. Am. Chem. Soc.* **1988**, *110*, 6119–6124.
(16) Perng, J.-H.; Duchowski, J. K.; Bocian, D. F. *J. Phys. Chem.* **1990**, *94*, 6684–6691.
(17) Girolami, G. S.; Milam, S. N.; Suslick, K. S. *J. Am. Chem. Soc.* **1988**, *110*, 2011–2012.
(18) Kim, K.; Lee, W. S.; Kim, H. J.; Cho, S. H.; Girolami, G. S.; Gorlin, P. A.; Suslick, K. S. *Inorg. Chem.* **1991**, *30*, 2652–2656.
(19) Bilsel, O.; Rodriguez, J.; Holten, D. *J. Phys. Chem.* **1990**, *94*, 3508–3512.
(20) Buchler, J. W.; De Cian, A.; Fischer, J.; Hammerschmitt, P.; Löffler, J.; Scharbert, B.; Weiss, R. *Chem. Ber.* **1989**, *122*, 2219–2228.
(21) Duchowski, J. K.; Bocian, D. F. *Inorg. Chem.* **1990**, *29*, 4158–4160.
(22) Bilsel, O.; Rodriguez, J.; Milam, S. N.; Gorlin, P. A.; Girolami, G. S.; Suslick, K. S.; Holten, D. *J. Am. Chem. Soc.* **1992**, *114*, 6528–6538.
(23) Radzki, S.; Mack, J.; Stillman, M. J. *New. J. Chem.* **1992**, *16*, 583–589.
(24) Buchler, J. W.; Kihn-Botulinski, M.; Löffler, J.; Scharbert, B. *New J. Chem.* **1992**, *16*, 545–553.
(25) Buchler, J. W.; Löffler, J.; Wicholas, M. *Inorg. Chem.* **1992**, *31*, 524–526.
(26) Buchler, J. W.; Kihn-Botulinski, M.; Löffler, J.; Wicholas, M. *Inorg. Chem.* **1989**, *28*, 3770–3772.
(27) Duchowski, J. K.; Bocian, D. F. *J. Am. Chem. Soc.* **1990**, *112*, 8807–8811.
(28) Lachkar, M.; De Cian, A.; Fischer, J.; Weiss, R. *New J. Chem.* **1988**, *12*, 729–731.
(29) Chabach, D.; Lachkar, M.; De Cian, A.; Fischer, J.; Weiss, R. *New J. Chem.* **1992**, *16*, 431–433.
(30) Moussavi, M.; De Cian, A.; Fischer, J.; Weiss, R. *Inorg. Chem.* **1986**, *25*, 2107–2108.

0002-7863/93/1515-8153$04.00/0

It has been shown that $M^{IV}(P)_2$ (where M is Ce, Zr, Hf, U, or Th) or $[M^{III}(P)_2]^-TBA^+$ (where P is the dianion of a given porphyrin ring, TBA^+ = tetra-*n*-butylammonium cation, and M is Y or a lanthanide metal) can be reversibly oxidized by up to four electrons or reversibly reduced by up to two electrons depending upon the specific metal ion, its oxidation state (M^{III} or M^{IV}), and the utilized electrochemical solvent.[10-17,27] Each reaction proceeds via stepwise one-electron transfers, and up to nine different oxidation states (one neutral, four oxidized and four reduced) may be obtained for a given double-decker complex in nonaqueous media. Most of the oxidized and reduced species have been generated only on the cyclic voltammetry time scale and, for this reason, very little is known with respect to the site of electron transfer and spectroscopic properties of other than neutral and singly oxidized forms of the complexes. Some of the electrode reactions can be associated with the central metal ion while others will involve either one or both porphyrin macrocycles.

Many singly oxidized double-decker complexes exhibit a large $\pi-\pi$ interaction between the two macrocycles.[2,5,10-15,18,20,28] This most often occurs for the bis(octaethylporphyrin) derivatives and results in a facile formation of the porphyrin π cation radical (i.e., an easier oxidation) as compared to a single macrocyclic species. The oxidized double-decker porphyrins exhibit a near-IR absorption band which is not present in the neutral complex,[3,6-8,13,14,17,21,22] and may also have diagnostic infrared marker bands indicative of a porphyrin π cation radical.[31-33] These bands generally appear between 1270 and 1295 cm^{-1} for monomeric tetraphenylporphyrins (TPP)[32,33] or between 1520 and 1570 cm^{-1} for octaethylporphyrins (OEP).[31,33] Similar bands have also been reported for singly oxidized $[M(TPP)_2]^+$ (M = Th or U)[17] and [M(OEP)(TPP)]$^+$ (M = Eu[14] or Ce[20]). The latter two cationic complexes have bands characteristic of an OEP rather than a TPP π cation radical, thus implying that localization of the hole is more on the OEP than on the TPP macrocycle.[14,20] On the other hand, resonance Raman spectra of $[Ce(OEP)(TPP)]^+$ are consistent with the electron having been abstracted from a mixed orbital involving both the OEP and TPP macrocycles.[21] This point might be resolved by a spectroscopic study of higher oxidized or reduced forms of double-decker complexes, but an analysis of this type has yet to appear in the literature.

Our laboratory previously reported the electrochemistry of single phthalocyanine[34] (Pc) and porphyrin[35,36] complexes containing U(IV) or Th(IV) central metals and we have now turned our attention to the electrochemical and spectroelectrochemical characterization of symmetrical and nonsymmetrical actinide double-decker porphyrins and phthalocyanines of the type $M(P)_2$, $M(Pc)_2$, M(P)(Pc), and M(P)(P′) where M = Th or U and P or P′ = the dianion of octaethylporphyrin, tetraphenylporphyrin, or tetra-*p*-tolylporphyrin (TpTP). Each compound is characterized as to its redox potentials, and these data are utilized to chemically or electrochemically generate new forms of the complex in higher or lower oxidation states which are then examined by ^1H NMR, ESR, IR, or UV–visible spectroscopy.

Experimental Section

Materials. HPLC grade dichloromethane (CH_2Cl_2) was first treated with sulfuric acid and then washed once with water, twice with sodium bicarbonate, and again twice with water. Next it was dried over magnesium sulfate and twice distilled under nitrogen, first over phosphorus pentoxide and then over calcium hydride. Toluene was twice treated with cold sulfuric acid and then washed once with water, twice with sodium bicarbonate, and again twice with water after which it was dried over calcium hydride and distilled over phosphorus pentoxide under nitrogen. Acetonitrile (CH_3CN) and pyridine (py) were distilled from CaH_2 under nitrogen. Tetra-*n*-butylammonium perchlorate, $TBA(ClO_4)$, was recrystallized from absolute ethanol and then dried and stored in a vacuum oven at 40 °C.

The synthesis of the investigated compounds is as follows:

U(OEP)(Pc). $U(OEP)Cl_2$[37] and $(Pc)Na_2$[38] were used as starting materials for the synthesis of U(OEP)(Pc); these compounds were prepared according to literature procedures after which they were heated under vacuum at 110 °C for 3 h prior to use. A 1-chloronaphthalene solution (30 mL) containing 0.38 g of $U(OEP)Cl_2$ (0.59 mmol) was added to 1.0 g of $Na_2(Pc)$ (2.68 mmol). The mixture was refluxed for 40 h under argon as the progress of the reaction was monitored by UV–vis spectroscopy. The mixture was then cooled and precipitated by addition of hexane. The crude product was filtered and dissolved in chloroform, and the solution was then concentrated and purified by column chromatography (SiO_2, 30 × 5 cm) with CH_2Cl_2/heptane (1:1) as eluent. A fraction containing trace $(OEP)H_2$ was eluted first. A second fraction containing U(OEP)(Pc) was then collected, and trace $U(Pc)_2$ was finally obtained. No $U(OEP)_2$ was detected. After evaporation, the crude solid was crystallized by addition of heptane to yield 0.34 g (45%) of U(OEP)(Pc). MS (DCI mode) ((*m*/*z*) ab. %): 1282 $(M + H)^+$, 100.

U(TPP)(Pc). U(TPP)(Pc) was synthesized according to the above procedure for U(OEP)(Pc) with 1.0 g of $U(TPP)Cl_2$[37] (1.08 mmol) and 1.5 g of $Na_2(Pc)$ (2.68 mmol) in 30 mL of 1-chloronaphthalene. Purification of the crude solid was achieved by column chromatography (silica gel, CH_2Cl_2/heptane). Evaporation of the major fraction yielded 0.44 g (30.0%) of U(TPP)(Pc). Minor fractions of free base $(TPP)H_2$ and $U(Pc)_2$ were also collected. MS (DCI mode) ((*m*/*z*) ab. %): 1362 $(M + H)^+$, 100.

U(TpTP)(Pc). U(TpTP)(Pc) was synthesized by following the method described above. $U(TpTP)Cl_2$ (1.5 g, 1.54 mmol) and $Na_2(Pc)$ (2 g, 3.58 mmol) gave 0.21 g of U(TpTP)(Pc) (20% yield). MS (FAB mode) ((*m*/*z*) ab. %): 1419 $(M + H)^+$, 100.

U(OEP)(TPP). U(OEP)(TPP) was synthesized from 0.56 mmol of $Li_2(OEP)$ (*in situ* preparation[39]) and 0.5 g (0.54 mmol) of $U(TPP)Cl_2$[37] according to the procedure given above for U(OEP)(Pc). After purification of column chromatography (silica gel, toluene/heptane 1:1) four fractions were separated. $U(OEP)_2$ was first eluted after which a second fraction containing a mixture of $(TPP)H_2$ and $(OEP)H_2$ was collected. $U(TPP)_2$ was present in trace amounts and was not recovered under the chromatographic conditions. The third fraction was identified as U(OEP)(TPP) of which 0.23 g was collected (30% yield). MS (FAB mode) ((*m*/*z*) ab. %): 1384 $(M + H)^+$, 100.

$U(OEP)_2$ and $U(TPP)_2$. The U(IV) bis-porphyrin complexes were synthesized according to the method of Girolami and Suslick.[9] $U(OEP)_2$: MS (DCI mode) ((*m*/*z*) ab. %) 1303 $(M + H)^+$, 100. $U(TPP)_2$: MS (FAB mode) ((*m*/*z*) ab. %) 1463 $(M + H)^+$, 100.

$U(Pc)_2$. The U(IV) bis(phthalocyanine) complex was obtained by using a method which was slightly modified from one described in the literature.[40] In this procedure, 3 g (5.38 mmol) of $Na_2(Pc)$ and 0.9 g (2.37 mmol) of UCl_4 were allowed to react in boiling 1-chloronaphthalene (30 mL) for 12 h. The solution was filtered while hot and, after cooling, the solid was precipitated from solution with heptane. Purification was achieved as described above for U(OEP)(TPP) and gave 0.25 g (7.4% yield) of $U(Pc)_2$. MS (FAB mode) ((*m*/*z*) ab. %): 1262 $(M + H)^+$, 100. Other spectroscopic data on this compound are in agreement with those previously reported.[40]

The seven double-decker thorium derivatives were synthesized in a similar manner as described above for uranium compounds having the same set of porphyrin and/or phthalocyanine macrocycles. The reactants involved in these syntheses as well as the final product yields are given below.

Th(OEP)(Pc): 1 g (1.20 mmol) of $Th(OEP)Cl_2$ and 2 g (3.58 mmol) of $Na_2(Pc)$ gave 0.40 g of Th(OEP)(Pc) (26% yield). MS (FAB mode) ((*m*/*z*) ab. %): 1276 $(M + H)^+$, 100.

(31) Kadish, K. M.; Mu, X. H. *Pure Appl. Chem.* **1990**, *62*, 1051.
(32) Scholz, W. F.; Reed, C. A.; Lee, Y. J.; Scheidt, W. R.; Lang, G. *J. Am. Chem. Soc.* **1982**, *104*, 6791–6793.
(33) Shimomura, E. T.; Phillippi, M. A.; Goff, H. M. *J. Am. Chem. Soc.* **1981**, *103*, 6778–6780.
(34) Guilard, R.; Dormond, A.; Belkalem, M.; Anderson, J. E.; Liu, Y. H.; Kadish, K. M. *Inorg. Chem.* **1987**, *26*, 1410–1414.
(35) Kadish, K. M.; Liu, Y. H.; Anderson, J. E.; Charpin, P.; Chevrier, G.; Lance, M.; Nierlich, M.; Dormond, A.; Belkalem, B.; Guilard, R. *J. Am. Chem. Soc.* **1988**, *110*, 6455–6462.
(36) Kadish, K. M.; Liu, Y. H.; Anderson, J. E.; Dormond, A.; Belkalem, M.; Guilard, R. *Inorg. Chim. Acta* **1989**, *163*, 201–205.
(37) Dormond, A.; Belkalem, B.; Charpin, P.; Lance, M.; Vigner, D.; Folcher, G.; Guilard, R. *Inorg. Chem.* **1986**, *25*, 4785–4790.
(38) Linstead, R. P.; Robertson, J. M. *J. Chem. Soc.* **1936**, 1736–1738.
(39) Arnold, J. *J. Chem. Soc., Chem. Commun.* **1990**, 976–978.
(40) Lux, F.; Dempf, D.; Graw, D. *Angew. Chem., Int. Ed. Engl.* **1968**, *7*, 819–820.

Th(TPP)(Pc): 1 g (1.09 mmol) of $Th(TPP)Cl_2$ and 2 g (3.58 mmol) of $Na_2(Pc)$ gave 0.34 g of Th(TPP)(Pc) (23% yield). MS (FAB mode) ((*m*/*z*) ab. %): 1357 $(M + H)^+$, 100.

Th(TpTP)(Pc): 1 g (1.03 mmol) of $Th(TpTP)Cl_2$ and 2 g (3.58 mmol) of $Na_2(Pc)$ gave 0.28 g of Th(TpTP)(Pc) (20% yield). MS (FAB mode) ((*m*/*z*) ab %): 1413 $(M + H)^+$, 100.

Th(OEP)(TPP): 0.60 g (0.66 mmol) of $Th(TPP)Cl_2$ and 0.67 mmol of $Li_2(OEP)$ (*in situ* preparation[39]) gave 0.14 g of Th(OEP)(TPP) (16% yield). MS (FAB mode) ((*m*/*z*) ab. %): 1379 $(M + H)^+$, 100.

$Th(OEP)_2$ and $Th(TPP)_2$. The Th(IV) bis-porphyrin complexes were synthesized according to the method of Girolami and Suslick.[9] $Th(OEP)_2$: MS (DCI mode) ((*m*/*z*) ab. %) 1297 $(M + H)^+$, 100. $Th(TPP)_2$: MS (FAB mode) ((*m*/*z*) ab. %) 1456 $(M + H)^+$, 100.

$Th(Pc)_2$. The Th(IV) bis(phthalocyanine) complex was obtained by using the method described above for $U(Pc)_2$. In a typical experiment, 3 g (5.38 mmol) of $Na_2(Pc)$ and 1.72 g (4.6 mmol) of $ThCl_4$ gave 0.18 g of $Th(Pc)_2$ (6.2% yield). MS (FAB mode) ((*m*/*z*) ab. %): 1257 $(M + H)^+$, 100.

Phenoxathiinylium Radical Cation. To a solution of 1 g (0.5 mmol) of phenoxathiin in 30 mL of CH_2Cl_2 under argon was added 4 mL (4 mmol) of a 1.0 M solution of $SbCl_5$ in CH_2Cl_2. The violet precipitate was collected by filtration and dried under vacuo, yielding quantitatively phenoxathiinylium hexachloroantimonate.

Oxidized Forms. Each neutral double-decker species was oxidized with phenoxathiinylium hexachloroantimonate[41] in CH_2Cl_2. The details for synthesis of each singly-oxidized species are as follows.

[U(TPP)Pc)][$SbCl_6$]: 39 mg (0.073 mmol) of phenoxathiinylium radical in 10 mL of CH_2Cl_2 were added dropwise to a solution of 100 mg (0.073 mmol) of U(TPP)(Pc) in 30 mL of CH_2Cl_2. Addition of heptane to the reaction mixture led to a crystalline powder. Filtration of the solid gave 60 mg of [U(TPP)Pc)][$SbCl_6$] (49% yield).

[U(OEP)Pc)][$SbCl_6$]: 100 mg (0.078 mmol) of U(OEP)(Pc) and 42 mg (0.078 mmol) of phenoxathiinylium radical gave 100 mg of [U(OEP)-Pc)][$SbCl_6$] (79% yield).

[$U(Pc)_2$][$SbCl_6$]: 100 mg (0.079 mmol) of $U(Pc)_2$ and 43 mg (0.079 mmol) of phenoxathiinylium radical gave 80 mg of [$U(Pc)_2$][$SbCl_6$] (63% yield).

[$U(OEP)_2$)][$SbCl_6$]: 50 mg (0.038 mmol) of $U(OEP)_2$ and 21 mg (0.038 mmol) of phenoxathiinylium radical gave 50 mg of [$U(OEP)_2$)]-[$SbCl_6$] (80% yield).

[U(OEP)(TPP)][$SbCl_6$]: 50 mg (0.036 mmol) of U(OEP)(TPP) and 19 mg (0.036 mmol) of phenoxathiinylium radical gave 25 mg of [U(OEP)-(TPP)][$SbCl_6$] (40% yield).

[Th(TPP)(Pc)][$SbCl_6$]: 100 mg (0.074 mmol) of Th(TPP)(Pc) and 39 mg (0.074 mmol) of phenoxathiinylium radical gave 60 mg of [Th-(TPP)(Pc)][$SbCl_6$] (48% yield).

[Th(OEP)(Pc)][$SbCl_6$]: 100 mg (0.078 mmol) of Th(OEP)(Pc) and 42 mg (0.078 mmol) of phenoxathiinylium radical gave 78 mg of [Th-(OEP)(Pc)][$SbCl_6$] (62% yield).

[$Th(Pc)_2$][$SbCl_6$]: 50 mg (0.040 mmol) of $U(Pc)_2$ and 22 mg (0.074 mmol) of phenoxathiinylium radical gave 50 mg of [$Th(Pc)_2$][$SbCl_6$] (79% yield).

[$Th(OEP)_2$][$SbCl_6$]: 30 mg (0.023 mmol) of $Th(OEP)_2$ and 12 mg (0.023 mmol) of phenoxathiinylium radical gave 25 mg of [$Th(OEP)_2$]-[$SbCl_6$] (66% yield).

[$Th(TPP)_2$][$SbCl_6$]: 40 mg (0.028 mmol) of $Th(TPP)_2$ and 15 mg (0.028 mmol) of phenoxathiinylium radical gave 40 mg of [$Th(TPP)_2$]-[$SbCl_6$] (81% yield).

[Th(OEP)(TPP)[$SbCl_6$]: 40 mg (0.029 mmol) of Th(OEP)(TPP) and 16 mg (0.029 mmol) of phenoxathiinylium radical gave 20 mg of [Th-(OEP)(TPP)][$SbCl_6$] (40% yield).

Preparation of Toluene/CH_3CN Solvent. Twenty milliliters of toluene was added to a flask containing 855 mg of $TBA(ClO_4)$. Some, but not all, of the supporting electrolyte dissolved, and 4 mL of acetonitrile was then added to solubilize $TBA(ClO_4)$ which was approximately 0.1 M. A cyclic voltammogram of this solution was then taken in order to ascertain the presence or absence of a cathodic wave around −2.35 V which was only present over a range of acetonitrile concentration between 18 and 22% in toluene. When this redox process was observed, a few drops of toluene were added to solution until the wave disappeared. Under these conditions the cathodic potential window could be extended to ~−2.7 V vs SCE.

The relative solution resistance of the above toluene/CH_3CN mixture was evaluated by measurement of the peak-to-peak separation, ΔE_p, for a given investigated compound. Whenever ΔE_p was greater than 100 mV for a known reversible process, a few drops of acetonitrile was added to the electrochemical cell in order to increase dissociation of the supporting electrolyte while at the same time maintaining the absence of the wave at −2.35 V. Under the final conditions, the concentration of CH_3CN was between 15 and 20%.

Instrumentation. All electrochemical measurements were carried out with a conventional three-electrode system. A glassy carbon disk of approximately 0.07 cm^2 surface area served as the working electrode, and a platinum wire was used as the counter electrode. The reference electrode was a homemade saturated calomel electrode (SCE) which was separated from the working solution by a fritted glass bridge. A gold minigrid electrode of the type described in the literature[42] was used for thin-layer spectroelectrochemical measurements. Controlled potential electrolyses were performed in an inert atmosphere drybox (Vacuum Atmosphere Co.) using an "H" type cell which had platinum gauge working and counter electrodes.

Differential pulse voltammetry was obtained with an IBM EC 225 2A voltammetric analyzer. Cyclic voltammetry was performed with an IBM EC 225 2A voltammetric analyzer or an EG&G Princeton Applied Research (PAR) Model 173 potentiostat coupled to an EG&G Model 175 universal programmer. IR compensation was used for both cyclic and differential pulse voltammetry. Current–voltage curves were recorded on an EG&G Model RE 0151 X-Y recorder. Controlled potential electrolyses were carried out on an EG&G Model 173 potentiostat equipped with an EG&G Model 179 digital coulometer to record the total charge transferred. Thin-layer spectroelectrochemical measurements were made with an EG&G Model 173 potentiostat coupled with a Tracor Northern TN-6500 spectrometer/multichannel analyzer to obtain time-resolved spectral data.

UV–visible spectra were obtained with an IBM 9430 or a Varian Cary I spectrophotometer. A Perkin-Elmer Model 330 spectrophotometer was used to record data in the near-infrared (near-IR) region. Infrared spectra of the solid samples were obtained as a 1% dispersion in CsI with a Nicolet 205 or a Bruker IFS 66 V FTIR spectrophotometer.

In-situ Fourier transform infrared (FTIR) measurements were carried out with a homemade light transparent spectroelectrochemical cell[42] using an IBM IR 32 spectrometer which was coupled with an IBM 9000 computer system and an EG&G Model 173 potentiostat.

ESR spectra were recorded on a Bruker Model ER 100D spectrometer equipped with an ER 040-X microwave bridge and an ER 080 power supply. The *g* values were measured relative to diphenylpicrylhydrazyl (DPPH) ($g = 2.0037 \pm 0.0002$). The spectrometer was equipped with a variable-temperature apparatus, and an Omega Model DR-41 RTD digital thermocouple was inserted into the cavity to monitor changes of temperature. Samples for ESR measurements were prepared inside the drybox and then stored in liquid nitrogen outside of the box.

^1H NMR spectra were recorded on a Bruker WM 400 spectrometer of the "Centre de Spectrométrie Moléculaire" at the University of Bourgogne. Spectra were measured in 0.5 mL of C_6D_6 with tetramethylsilane as a reference.

Mass spectra were obtained on a Kratos Concept 32 S of the "Centre de Spectrométrie Moléculaire" at the University of Bourgogne in the positive DCI mode (desorption chemical ionization) (NH_3 reactant gas) or in the positive FAB mode (fast atom bombardment) (*m*-nitrobenzyl alcohol as matrix).

Results and Discussion

Synthesis. Two major syntheses of uranium and thorium double-decker porphyrins and phthalocyanines have been reported in the literature,[9,40] but slightly different procedures were used in the present study due to the low yields obtained with these methods. For example, the "one pot" reaction of MI_4 and phthalodinitrile gives $M(Pc)_2$ (M = U or Th),[40] but the yield was improved in this present study by reacting $Na_2(Pc)$ with MCl_4 in boiling 1-chloronaphthalene (eq 1).

$$2Na_2(Pc) \xrightarrow[MCl_4,\ \text{reflux}]{\text{1-chloronaphthalene}} M(Pc)_2 \qquad (1)$$

M = Th, U

Our initial synthesis of the homoleptic porphyrins also followed a literature method[9] but low yields were again obtained, perhaps

(41) Gans, P.; Marchon, J. C.; Reed, C. A.; Regnard, J. R. *Nouv. J. Chim.* **1981**, *5*, 203.

(42) Lin, X. Q.; Kadish, K. M. *Anal. Chem.* **1985**, *57*, 1498.

Table I. Spectral Data for Neutral Double-Decker Thorium and Uranium Complexes in CH_2Cl_2

metal	macrocycles		λ, nm (10^{-4} ε, dm^3 mol^{-1} cm^{-1})							
			Pc	Soret		Q″	Q′			NIR
Th	Pc	Pc[a]	330 (12.4)				585 (sh)	640 (18.4)	689 (sh)	
		OEP	340 (9.6)		393 (9.4)	466 (2.4)	570 (sh)	608 (2.9)		731 (0.1)
		TPP	333 (6.1)	350 (sh)	412 (14.9)	479 (2.6)	575 (1.4)	624 (1.7)	700 (sh)	791 (1.5)
		TpTP	330 (9.0)		412 (21.6)	480 (4.6)	577 (sh)	627 (2.3)	700 (w)	791 (2.7)
	OEP	OEP		345 (sh)	383 (14.2)	470 (sh)	535 (0.2)	577 (0.8)	644 (w)	
		TPP		350 (sh)	392 (37.3)	483 (1.3)	542 (1.4)	581 (0.6)	636 (br,w)	
	TPP	TPP			400 (53.9)	480 (1.4)	546 (1.2)	600 (0.6)		
U	Pc	Pc[a]	332 (6.9)				593 (sh)	638 (9.0)	700 (2.1)	
		OEP	338 (10.1)		393 (6.8)	466 (2.6)	575 (sh)	619 (3.3)		870 (0.8,br)
		TPP	332 (8.5)		412 (10.3)	481 (3.7)	582 (1.6)	636 (2.3)	745 (sh)	829 (1.4)
		TpTP	336 (8.6)		413 (11.0)	482 (4.2)	587 (sh)	637 (2.3)	684 (w)	827 (1.5)
	OEP	OEP		350 (sh)	386 (16.6)	464 (2.2)	539 (0.9)	582 (1.9)	668 (0.6)	
		TPP		350 (sh)	396 (19.4)	491 (0.9)	549 (1.0)	586 (0.5)	638 (br,w)	
	TPP	TPP			402 (28.0)	488 (2.3)	549 (1.5)	619 (0.7)		

[a] In pyridine. sh = shoulder; w = weak; br = broad.

due to the low stability of the $M(NEt_2)_4$ metalating agent toward light and air. It was later observed that the nonsymmetrical derivatives could be obtained in higher yields from the reaction of $M(P)Cl_2$ (M = Th, or U) and $Li_2(P)$ or $Li_2(Pc)$ in refluxing 1-chloronaphthalene, and this procedure was utilized in all future syntheses of these compounds (eqs 2 and 3).

$$M(P)Cl_2 + M'_2(P') \xrightarrow[\text{reflux}]{\text{1-chloronaphthalene}} M(P)(P') + 2M'Cl \quad (2)$$

P = TPP, OEP; P′ = TPP, OEP; M = Th, U; M′ = Li, Na

$$M(P)Cl_2 + M'_2(Pc) \xrightarrow[\text{reflux}]{\text{1-chloronaphthalene}} M(P)(Pc) + 2M'Cl \quad (3)$$

P = TPP, OEP, TpTP; M = Th, U; M′ = Li, Na

Trace amounts of both the free base porphyrin and the symmetrical $M(P')_2$ complexes (where P′ comes from $Li_2(P')$ or $Na_2(P')$) are formed in the above reaction, but formation of the symmetrical $M(P)_2$ derivatives (where P comes from $M(P)Cl_2$) was never observed. Also, the molecular ion was either the most abundant ion or the only ion present in the mass spectrum when the compounds were characterized by mass spectrometry with use of either the DCI or FAB techniques. This result is in good agreement with the known high stability of homoleptic and heteroleptic double-decker porphyrins and phthalocyanines.

UV–Visible Spectra of Neutral Compounds. UV–visible spectra of $M(OEP)_2$, $M(TPP)_2$, and M(OEP)(TPP) have been presented in the literature for complexes containing Hf,[11] Zr,[11,18] Ce,[1-7,15,19-21,23,28,29] Th,[8,17,22] and U[9,17] metal ions. The spectra of the symmetrical double-decker porphyrins have only a single Soret band, and this is also the case for most of the nonsymmetrical M(OEP)(TPP) derivatives whose Soret bands are located at wavelengths roughly half-way between those of the symmetrical $M(TPP)_2$ and $M(OEP)_2$ complexes having the same metal ion.

Separate UV–visible bands attributable to each individual macrocycle are also seen for the nonsymmetrical M(P)(Pc) derivatives which have spectral characteristics that can be assigned to both the phthalocyanine and porphyrin macrocyclic unit. This is illustrated in Figure 1 which shows the spectra of $U(TPP)_2$, U(TPP)(Pc), and $U(Pc)_2$ in CH_2Cl_2. The Soret band of U(TPP)(Pc) is located at 412 nm, and this value can be compared to a Soret band at 402 nm for $U(TPP)_2$ (Figure 1) or 420 nm for $U(TPP)(acac)_2$[37] (not shown). U(TPP)(Pc) exhibits a high-intensity band of the Pc unit at 332 nm, and this value is identical with λ_{max} for the Pc band of $U(Pc)_2$ (see Figure 1). Both peak maxima are blue shifted with respect to the corresponding Pc band of $U(Pc)(acac)_2$ which is located at 351 nm.[27] The Soret (porphyrin) and phthalocyanine absorption bands of M(OEP)(Pc) also show similar shifts compared to the UV–visible bands of $M(OEP)(acac)_2$ and $M(Pc)(acac)_2$ (see Table I).

Bilsel *et al.*[19] have suggested that the observed blue shifts in λ_{max} upon going from a monomacrocycle species to a double-decker complex with the same metal ion cannot be accounted for by simple exciton theory in the symmetrical double-decker derivatives. This is because the theory does not take into account orbital overlap between the two macrocycles (which are separated by a metal ion) and thus cannot explain those spectral features not observed in the related monomeric derivatives containing a single π-ring system.

The double-decker complexes all have a well-defined band at around 480 nm which derives from orbital overlap between the π systems of the two moieties and must involve transitions of orbitals delocalized over both macrocycles. The complexes can thus be described as a kind of supermolecule whose orbitals are formed by a linear combination of each ligand orbital and which has some transitions only seen in the double-decker species. For example, two new bands, labeled as Q′ and Q″,[8,43] appear at 630–650 and 480–500 nm, respectively. The position of these two bands strongly depends on the interspacing between the two macrocycles, i.e. on the size of the central metal ion.[22] This is illustrated in Figure 2 which shows the UV–visible spectra of U(OEP)(TPP) and Th(OEP)(TPP). Both compounds have well-defined Q′ and Q″ bands, and these are red shifted by ≈8 nm for U(OEP)(TPP) as compared to the analogous Th(OEP)(TPP) derivative, in accordance with the smaller ionic radius of the U^{IV} cation. A similar trend is also observed between the other Th and U double-decker species (see Table I) whose spectra can be compared with those of Zr, Hf, and Ce bis-porphyrinates.[1,2,11,20,28,44]

^{1}H NMR of Neutral Compounds. ^{1}H NMR data of the investigated neutral complexes are reported in Table II. Each $U(P)_2$, U(P)(P′), and U(P)(Pc) species exhibits ^{1}H NMR features typical of a paramagnetic complex, and this is shown in Figure 3 for U(OEP)(Pc) in C_6D_6 at 25 °C. The meso protons of the OEP unit appear as a broad signal at –6.30 ppm. The methyl proton resonance appears as a triplet at –2.80 ppm while the α-CH_2 protons of the same ethyl groups have resonances at –2.20 and –3.60 ppm. The two proton sites of the phthalocyanine ring show resonances at 5.67 and 4.17 ppm and these signals are attributed respectively to the H_α and H_β phthalocyanine protons which are shielded compared to the corresponding proton resonances of $U(Pc)(acac)_2$ at 6.73 and 5.86 ppm.[34] These data are in accordance with the resulting upfield shift of the meso protons when the two $acac^-$ ligands of $U(OEP)(acac)_2$ (–1.48 ppm)[37] are replaced by a Pc moiety to give U(OEP)(Pc) (–6.30 ppm). The methylenic and methylic protons of U(OEP)(Pc) are upfield shifted from the corresponding resonances of U(OEP)-

(43) Bilsel, O.; Buchler, J. W.; Hammerschmitt, P.; Rodriguez, J.; Holten. D. *Chem. Phys. Lett.* **1991**, *182*, 415–421.
(44) Buchler, J. W.; De Cian, A.; Elschner, S.; Fischer, J.; Hammerschmitt. P.; Weiss. R. *Chem. Ber.* **1992**, *125*, 107–115.

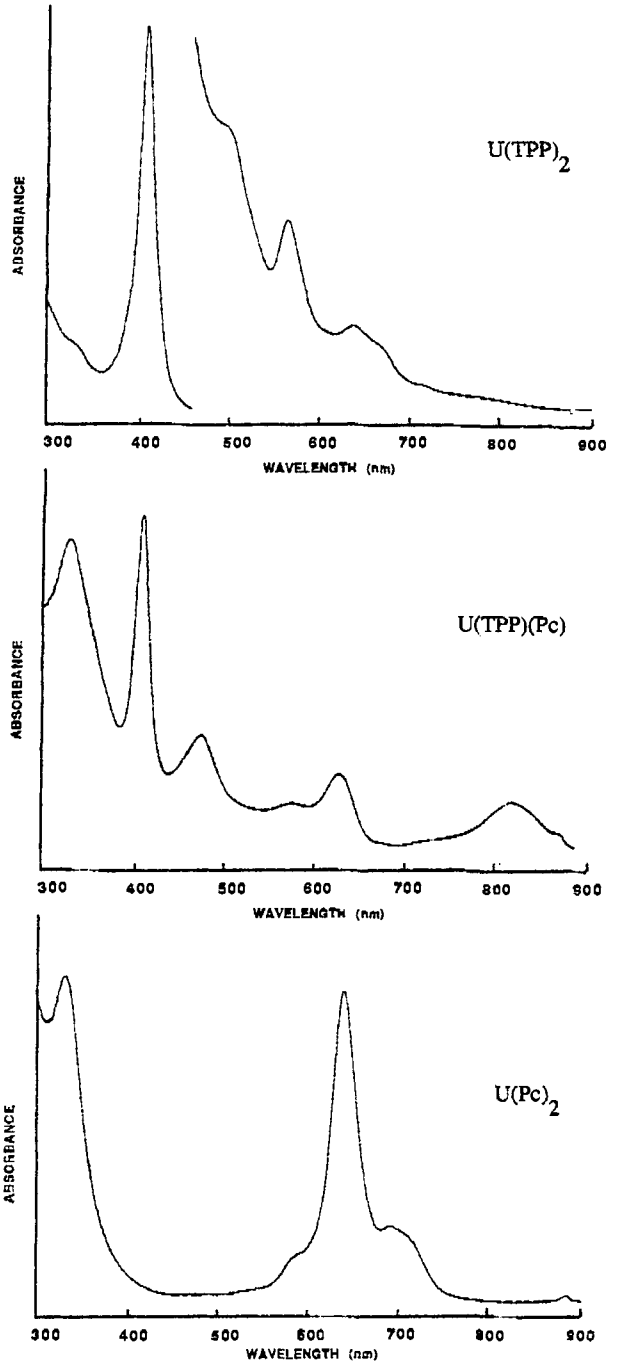

Figure 1. UV–visible spectra of $U(TPP)_2$, U(TPP)(Pc), and $U(Pc)_2$ in CH_2Cl_2.

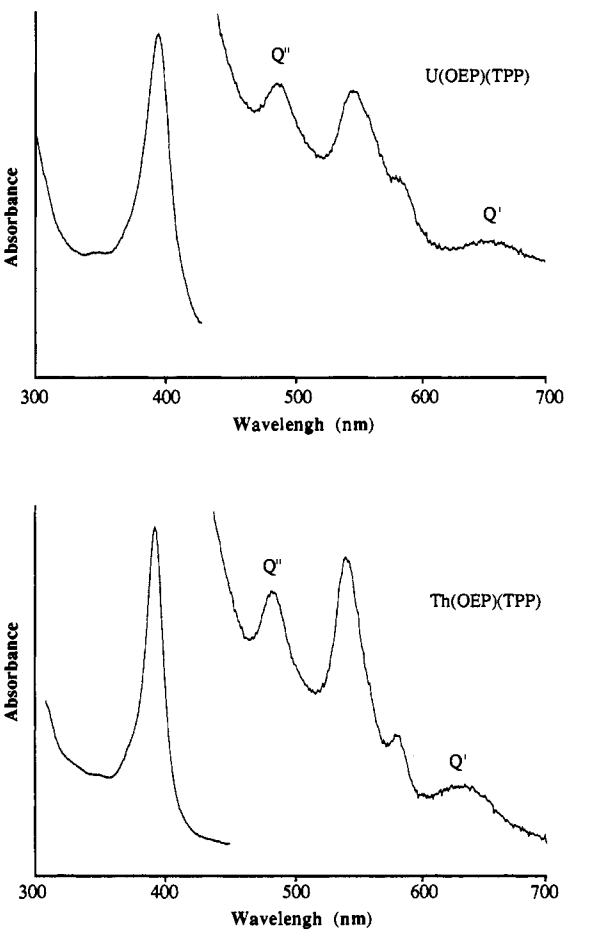

Figure 2. UV–visible spectra of Th(OEP)(TPP) and U(OEP)(TPP).

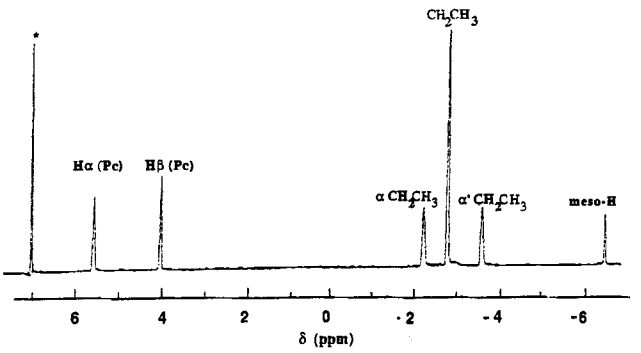

Figure 3. ^1H NMR spectrum of U(OEP)(Pc) in C_6D_6 at 25 °C.

$(acac)_2$ which are located at –0.31/–1.38 and –0.85 ppm, respectively.[37] The same effect can be noted for the α-CH_2 and β-CH_3 protons of U(OEP)(TPP) which are observed at –0.87, –3.06, and –0.05 ppm, respectively. A similar shift in the resonances was reported for Ce(OEP)(TPP)[20] and was attributed to the mutual influence of TPP and OEP on each other in this mixed macrocyclic complex. The same type of interaction seems to occur for the three investigated uranium phthalocyanine–porphyrin complexes which also induces a similar shielding.

The overall NMR data are consistent with the UV–visible data in that they demonstrate the sandwich structures of U(P)(Pc) and U(P)(P'). Such a structural geometry also explains diastereotopic resonances for the α-CH_2 and β-CH_3 protons of U(OEP)(Pc) which exhibit an ABR_3 multiplet. The signal at –2.20 ppm can be attributed to the exo protons of the α-CH_2 group. It is interesting to note that no significant changes in the chemical shifts are observed upon going from $U(OEP)_2$ or $U(TPP)_2$ to the mixed U(OEP)(TPP) complex. Five signals are obtained for the phenyl protons of the TPP rings on U(TPP)(OEP), and this is in accordance with a slow phenyl ring rotation on this time scale. Moreover, the "endo" ortho proton resonances at –3.91 to –6.5 ppm for $U(TPP)_2$, U(OEP)(TPP), or U(TPP)(Pc) are in all three cases strongly shielded due to the presence of the paramagnetic U(IV) atom.

All of the Th double-decker complexes exhibit signals within the range of 0–10 ppm. For example, the ^1H NMR spectrum of Th(OEP)(TPP) shows a single meso-proton signal at 9.24 ppm and two quartets at 4.17 and 3.86 ppm for the α-CH_2 protons of the OEP moiety. The splitting of the α-CH_2 resonance signal into two quartets can be easily explained by the strong anisochrony of these protons induced by the geometry of the molecule. The β-CH_3 protons of Th(OEP)(TPP) appear as a triplet at 1.41 ppm, and a slight shielding is observed for the pyrrole protons (δ = 8.23 ppm) compared to such a proton site in the octaeth-

Table II. ^{1}H NMR Data for Neutral and Singly-Oxidized Complexes at 25 °C in $CDCl_3$

	Pc protons				OEP protons						TPP protons									
	α-H		β-H		meso-H		α-CH_2		β-CH_3		Pyr-H		o-H		m-H		p-H		p-CH_3	
compd	m/i[b]	δ, ppm	m/i[b]	δ, ppm	m/i[b]	δ, ppm	m/i[b]	δ, ppm	m/i[b]	δ, ppm	m/i[b]	δ, ppm	m/i[b]	δ, ppm	m/i[b]	δ, ppm	m/i[b]	δ, ppm	m/i[b]	δ, ppm
U(OEP)(Pc)[a]	dd/8	5.67	dd/8	4.17	s/4	−6.30	m/8	−2.20	t/24	−2.80										
							m/8	−3.60												
[U(OEP)(Pc)]$^+$	s/8	−10.67	s/8	−20.60	s/4	11.80	s/8	10.76	t/24	0.05										
							s/8	6.19												
U(TPP)(Pc)	dd/8	6.06	dd/8	4.18							s/8	3.67	d/4	9.38	d/4	6.90	t/4	5.42		
													d/4	−6.50	d/4	3.26				
[U(TPP)(Pc)]$^+$	s/8	−10.68	s/8	−15.82							s/8	−30.79	s/4	10.30	s/4	5.59	t/4	6.41		
													s/4	−4.30	s/4	2.51				
U(TpTP)(Pc)	dd/8	6.17	dd/8	4.27							s/8	3.67	d/4	9.12	d/4	6.66			s/12	1.06
													d/4	−6.50	d/4	3.07				
U(OEP)(TPP)					s/4	−4.58	m/8	−0.87	t/24	−0.05	s/8	3.68	s/4	9.31	s/4	6.91	t/4	5.56		
							m/8	−3.06					s/4	−3.92	s/4	3.89				
[U(OEP)(TPP)]$^+$					s/4	29.70	s/8	19.70	t/24	2.48	s/8	−16.43	s/4	11.40	s/4	6.13	t/4	6.61		
							s/8	14.60					s/4	−0.95	s/4	3.90				
$U(Pc)_2$	m/8	4.89	m/8	3.53																
$[U(Pc)_2]^+$	m/8	3.54	m/8	3.40																
$U(TPP)_2$											s/16	4.58	s/8	9.83	s/8	7.15	t/8	5.67		
													s/8	−3.91	s/8	3.82				
$[U(TPP)_2]^+$											s/16	−5.48	m/8	8.96	m/8	8.96	t/8	6.17		
													d/8	2.40	brs/8	4.61				
$U(OEP)_2$					s/8	−4.68	q/16	−1.01	t/48	−0.67										
							q/16	−2.87												
$[U(OEP)_2]^+$					s/8	21.27	m/8	15.66	t/48	1.79										
							m/8	10.10												
Th(OEP)(Pc)[a]	dd/8	9.36	dd/8	7.96	s/8	9.42	m/16	3.7	t/24	2.00										
Th(TPP)(Pc)	dd/8	9.26	dd/8	8.26							s/8	8.39	m/4	7.62	brs/8	7.21	m/4	7.62		
													d/4	6.63						
Th(TpTP)(Pc)	dd/8	9.24	dd/8	8.25							s/8	8.39	d/4	7.44	d/4	7.09			s/12	2.63
													d/4	6.52	d/4	7.02				
Th(OEP)(TPP)					s/4	9.24	q/8	4.17	t/24	1.41	s/8	8.23	d/4	9.48	brs/8	8.23	t/8	7.75		
							q/8	3.86					d/4	6.64	brs/8	7.28				
$Th(Pc)_2$	dd/16	9.06	dd/16	8.31																
$Th(TPP)_2$											s/16	8.31	brs/8	9.35	m/8	8.05	t/8	7.72		
													brs/8	6.60	m/8	7.19				
$Th(OEP)_2$					s/4	9.42	q/8	4.02	t/24	2.00										
							q/8	3.08												

[a] In C_6D_6. [b] Key: dd = double doublet, s = singlet, d = doublet, t = triplet, q = quartet, brs = broad singlet.

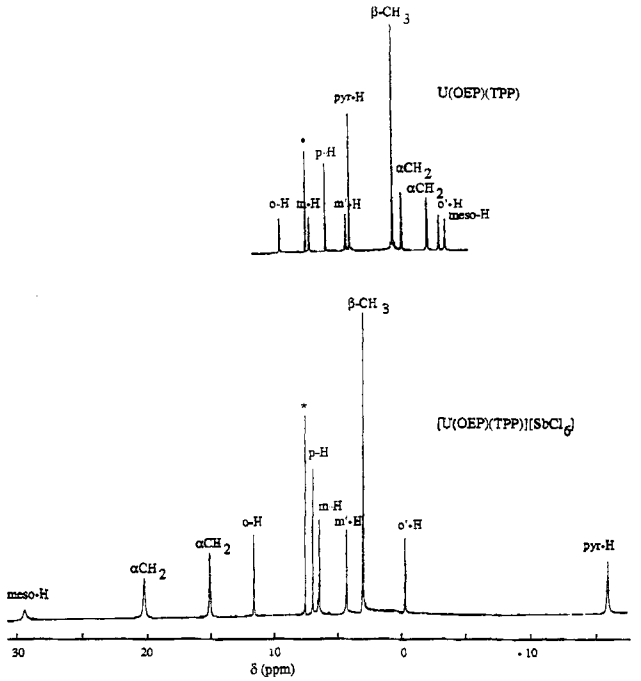

Figure 4. ^{1}H NMR spectrum of U(OEP)(TPP) and $[U(OEP)(TPP)]^+$-$[SbCl_6]^-$ in $CDCl_3$ at 25 °C.

Table III. Half-Wave Potentials (V vs SCE) for Oxidation and Reduction of Double-Decker Derivatives at a Glassy Carbon Electrode in CH_2Cl_2 Containing 0.1 M $TBA(ClO_4)$[a]

metal	macrocycles		oxidation			reduction		
			3rd	2nd	1st	1st	2nd	3rd
Th	OEP	OEP	1.91[b,c]	0.85	0.32	−1.53		
	OEP	TPP	1.65	1.05	0.55	−1.40	−1.73	
	TPP	TPP	1.79[b,c]	1.13	0.79	−1.27	−1.55	
	Pc	Pc		1.09[b,c]	0.74[b]	−0.57	−0.85	−1.36
	Pc	OEP	1.87[b,c]	1.02	0.50	−0.94	−1.38	−2.02[b]
	Pc	TPP	1.88[b,c]	1.22	0.66	−0.84	−1.27	−1.68
	Pc	TpTP	1.87[b,c]	1.17	0.64	−0.87	−1.30	−1.71
U	OEP	OEP	1.50	0.79	0.23	−1.55		
	OEP	TPP	1.62	0.98	0.46	−1.42	−1.76	
	TPP	TPP	1.78[b,c]	1.10	0.71	−1.27	−1.57	
	Pc	Pc		1.09[b,c]	0.74[b]	−0.56	−0.87	−1.38
	Pc	OEP	1.63	0.96	0.44	−0.92	−1.36	−1.98[b]
	Pc	TPP	1.74[b,c]	1.16	0.63	−0.82	−1.27	−1.69
	Pc	TpTP	1.72[b,c]	1.14	0.60	−0.86	−1.30	−1.76

[a] Potentials of $M(Pc)_2$ were measured in py containing 0.1 M $TBA(ClO_4)$ due to insolubility in CH_2Cl_2. [b] Peak potential obtained at a scan rate of 0.1 V/s. [c] Peak consists of overlapping processes.

ylporphyrin series. Similar behavior is observed for Th(OEP)-(TPP) and Th(TPP)(Pc). Also, the phenyl group of the TPP ring in Th(OEP)(TPP) shows five signals at 9.48, 8.23, 7.75, 7.28, and 6.64 ppm (see Table II).

^{1}H NMR of Singly-Oxidized Complexes. The ^{1}H NMR spectrum of each neutral uranium derivative changes dramatically upon oxidation. It was previously reported[17] that NMR spectra cannot be obtained for $[Th(TPP)_2]^+$, and this is also the case for the singly-oxidized $[Th(P)(P')]^+$ and $[Th(P)(Pc)]^+$ complexes investigated in this present study. On the other hand, the singly-oxidized U(IV) derivatives show well-defined ^{1}H NMR spectra, and this is illustrated in Figure 4 which shows the spectra of neutral and singly-oxidized U(OEP)(TPP) in C_6D_6 at 25 °C.

The abstraction of one electron from the neutral complex leads to a shift of the meso-H signal resonance from −4.58 to +29.70 ppm. The oxidized complex also shows a large deshielding (ca. 15 ppm) of the α-CH_2 protons while the β-CH_3 protons are deshielded by only ≈2.5 ppm. This result is in agreement with a charge delocalization on the OEP moiety. The pyrrole protons

Table IV. Half-Wave Potentials (V vs SCE) for Oxidation and Reduction of Double-Decker Derivatives at a Glassy Carbon Electrode in a Toluene/Acetonitrile Mixture (~8:2) Containing 0.1 M $TBA(ClO_4)$

metal	macrocycles		oxidation			reduction			
			3rd	2nd	1st	1st	2nd	3rd	4th
Th	OEP	OEP	1.63	0.80	0.39	−1.50	−1.82	−2.47	
	OEP	TPP	1.63	1.06	0.65	−1.31	−1.65	−2.19	−2.60[a]
	OEP	Pc		1.06	0.61	−0.86	−1.29	−1.85	−2.30[a]
	Pc	Pc			*b*	−0.63	−0.88	−1.36	−1.57
	Pc	TpTP		1.24	0.73	−0.83	−1.27	−1.70	−2.29[a]
U	OEP	OEP	*b*	0.72	0.33	−1.44	−1.82	−2.53	
	OEP	TPP	1.60	1.00	0.57	−1.32	−1.66	−2.17[a]	−2.23
	OEP	Pc	1.57	0.97	0.50	−0.91	−1.32	−1.96	−2.40[a]
	Pc	Pc			*b*	−0.65	−0.89	−1.39	−1.62
	Pc	TpTP		1.20	0.68	−0.82	−1.26	−1.69	−2.05[a]

[a] Peak potential obtained at a scan rate of 0.1 V/s. [b] Oxidations could not be obtained due to adsorption.

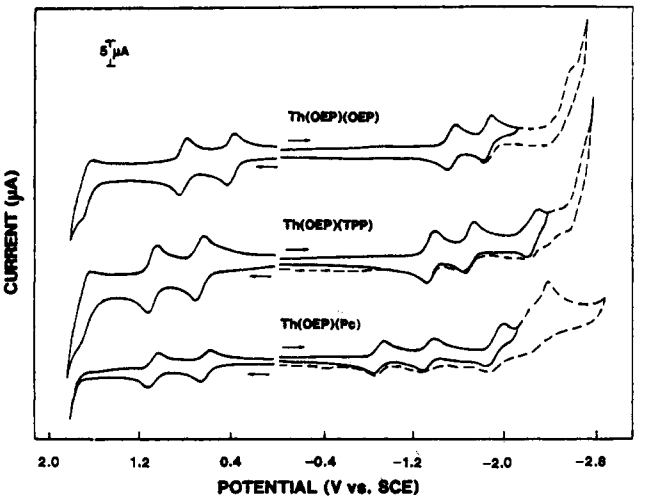

Figure 5. Cyclic voltammograms of $Th(OEP)_2$, Th(OEP)(TPP), and Th(OEP)(Pc) in a toluene/acetonitrile (~8:2) mixture containing 0.1 M $TBA(ClO_4)$. Scan rate = 0.1 V/s.

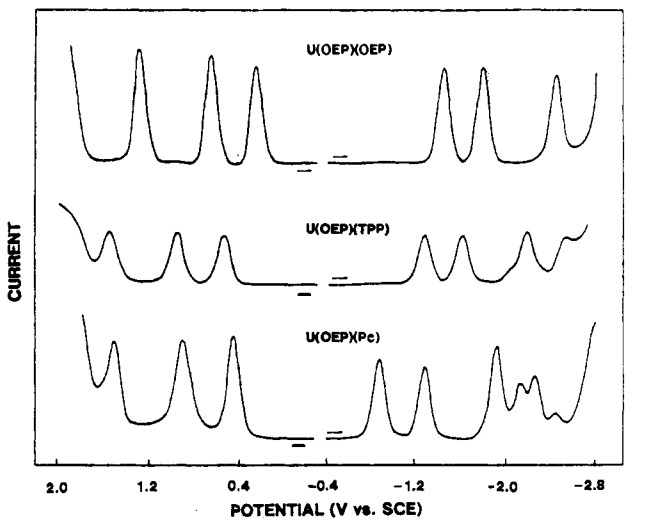

Figure 6. Differential-pulse voltammograms of $U(OEP)_2$, U(OEP)(TPP), and $U(TPP)_2$ in a toluene/acetonitrile (~8:2) mixture containing 0.1 M $TBA(ClO_4)$.

of the TPP group in $[U(OEP)(TPP)]^+$ are strongly shielded (≈19 ppm) but the phenyl protons of the complex are not greatly affected by the one-electron oxidation, which leads to the conclusion that the unpaired spin on the oxidized complex is partially transferred to the TPP ring. The ^{1}H NMR data agree with literature results on similar double-decker complexes[17,20,28] and provide additional

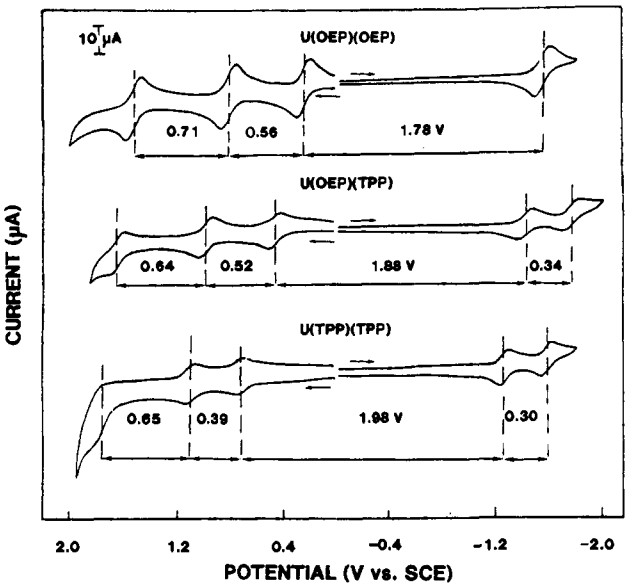

Figure 7. Cyclic voltammograms illustrating HOMO-LUMO gap and other potential differences in $E_{1/2}$ for the stepwise oxidation and reduction of $U(OEP)_2$, U(OEP)(TPP), and $U(TPP)_2$ in CH_2Cl_2 containing 0.1 M $TBA(ClO_4)$. Scan rate = 0.1 V/s.

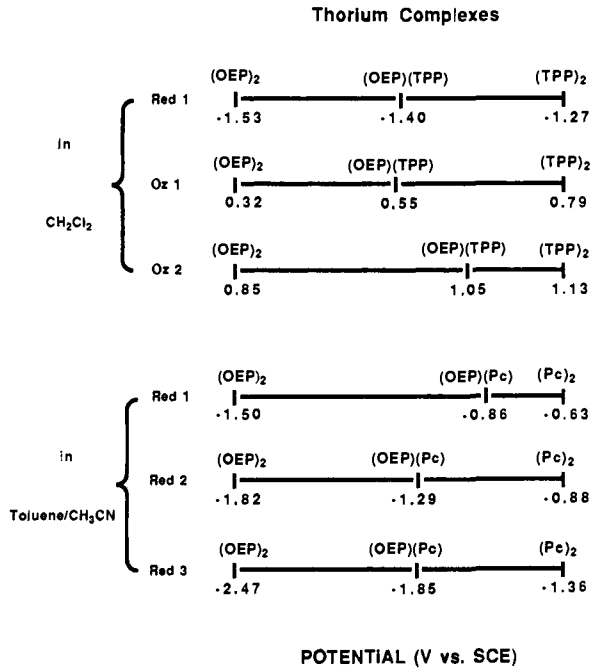

Figure 8. Comparison of half-wave potentials between Th(OEP)(TPP) or Th(OEP)(Pc) and the related homoleptic $Th(OEP)_2$, $Th(TPP)_2$, or $Th(Pc)_2$ derivatives. The listed potentials are taken from Tables III and IV.

proof that the abstracted electron comes from an orbital which involves both the TPP and the OEP rings rather than only one of the two macrocycles.

Another interesting feature of the NMR spectra is that deshielding is much larger for the OEP protons in oxidized U(OEP)(TPP) or $U(OEP)_2$ as compared to deshielding in the neutral species. The same trend is noted for the TPP protons of the singly-oxidized species which are more shielded in the heteroleptic U(OEP)(TPP) complex than in the homoleptic $U(TPP)_2$ derivative. All of these data are summarized in Table II.

Electrochemistry. The redox potentials of each double-decker complex were measured prior to controlled potential oxidation or reduction to generate a compound in a given oxidation state.

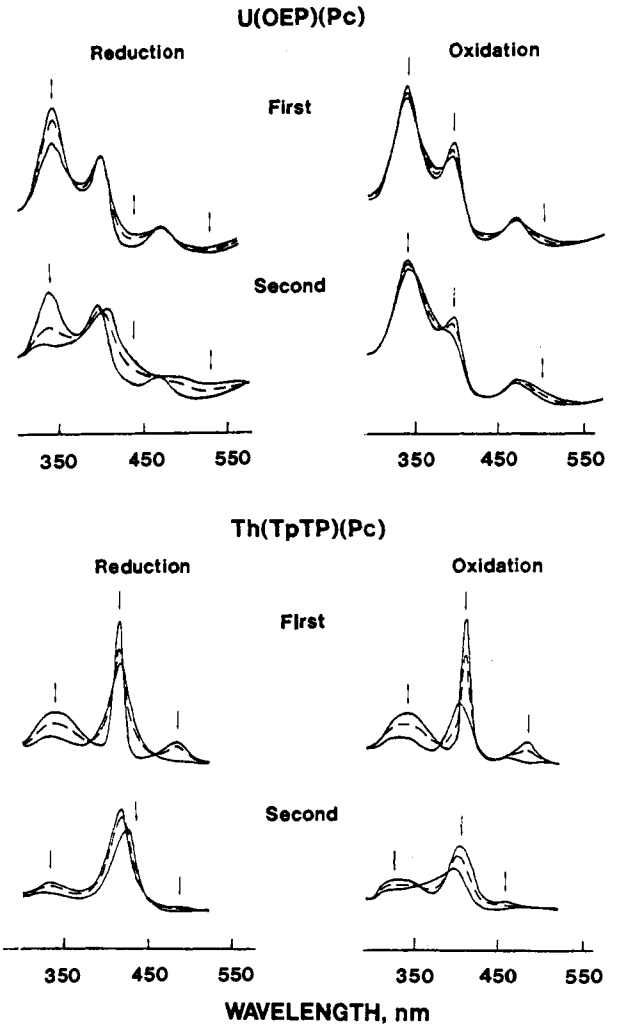

Figure 9. Electronic absorption spectra obtained during the first two oxidations and the first two reductions of U(OEP)(Pc) and Th(TpTP)(Pc) in CH_2Cl_2 containing 0.2 M $TBA(ClO_4)$.

Values of $E_{1/2}$ were obtained in CH_2Cl_2, a toluene/CH_3CN mixture, or both depending upon the solubility of the compounds. These data are summarized in Tables III and IV. The compounds with one or two porphyrin rings are all soluble in CH_2Cl_2 and, except for $M(TPP)_2$ and M(TPP)(Pc), are also soluble in the toluene/CH_3CN mixture. The $M(Pc)_2$ complexes are only slightly soluble in toluene/CH_3CN and their oxidation is poorly defined in this solvent, due in large part to the presence of adsorption at the electrode surface. On the other hand, $M(Pc)_2$ is quite soluble in pyridine containing 0.1 M $TBA(ClO_4)$ and, under these solution conditions, undergoes three reversible electroreductions and two irreversible oxidations.

Each double-decker derivative with at least one porphyrin ring undergoes three oxidations and either one, two, or three reductions in CH_2Cl_2 (see Table III). The toluene/acetonitrile mixture (~8:2) has a larger negative potential window (~2.7 V) than does CH_2Cl_2 (~2.0 V), and additional electroreductions can thus be observed in the mixed solvent system (see Table IV). Similar behavior is observed for U and Th complexes having the same set of porphyrin and/or phthalocyanine macrocycles, but the U derivatives are easier to oxidize than the Th derivatives by 30 to 110 mV depending upon the specific electrode reaction. The U(IV) complexes are also more difficult to reduce than the Th(IV) species, but the difference in potentials is smaller in this case and amounts to a maximum of 50 mV, depending upon the electrode reaction. U(IV) has two more electrons than does Th(IV), but its ionic radius is smaller which allows for a closer

Table V. UV–Visible Spectral Data of Neutral and Electrogenerated Thorium Double-Decker Complexes in CH_2Cl_2 Containing 0.2 M TBA(ClO_4)

macrocycles		charge	λ, nm (10^{-4} ε, dm^3 mol^{-1} cm^{-1})								
			Pc	Soret		Q″		Q′		NIR	
Pc	Pc[a]	0	338 (12.4)					592 (2.6)	646 (18.4)		
		−1	341 (12.4)					589 (9.2)	645 (6.5)	780 (1.5)	
		−2	341 (8.3)					558 (10.0)	583 (8.7)	854 (0.8)	
Pc	TPP	0	337 (6.1)		413 (14.9)	482 (2.6)		581 (1.4)	623 (1.7)	700 (sh)	787 (1.5)
		+1	332 (5.4)	405 (10.9)	416 (11.7)	456 (1.6)	512 (1.2)		650 (sh)	796 (0.5)	980 (0.4)	1300 (0.2, br)
		+2	320 (sh)		393 (12.9)	441 (4.2)	507 (1.4)			711 (0.8)	980 (0.4)	1300 (0.2, br)
		−1	337 (2.4)		416 (15.7)	492 (1.7)		546 (1.7)	595 (1.7)	627 (1.9)		
		−2	331 (3.2)		425 (16.3)	510 (3.3)		541 (3.3)	612 (3.0)		860 (w, br)	
Pc	OEP	0	340 (9.6)		393 (9.4)	466 (2.4)		570 (sh)	608 (2.9)		819 (1.1)	
		+1	340 (8.2)		391 (7.7)	466 (1.3)		558 (2.2)	625 (sh)	728 (0.1)	1075 (0.3, br)	1600 (0.6, br)
		+2	341 (7.3)		388 (5.9)	471 (0.8)			630 (sh)		1080 (0.2, br)	1600 (0.4, br)
		−1	339 (7.6)		393 (9.2)	466 (1.5)		536 (sh)	587 (2.3)	610 (2.4)	819 (w)	
		−2	339 (6.6)		393 (8.5)	466 (1.3)		537 (2.3)	579 (2.5)	618 (br)		
Pc	TpTP	0	340 (9.0)		412 (21.6)	482 (4.6)		585 (2.3)	604 (2.4)	623 (2.3)	718 (0.7)	799 (2.7)
		+1	322 (4.2)	347 (4.0)	404 (9.5)	460 (1.2)				723 (w)		
		+2	320 (3.0)		397 (5.9)			613 (2.0)	706 (1.5)	739 (1.4)		
		−1	334 (3.9)		414 (15.4)			547 (2.3)	599 (2.3)	633 (2.5)		
		−2	331 (2.5)		425 (12.4)			512 (3.1)	547 (3.0)	613 (2.6)		
TPP	TPP	0			401 (53.9)	481 (sh)		549 (1.2)	606 (0.6)			
		+1			399 (29.1)						800 (0.1)	1475 (0.4, br)
		+2			388 (18.7)	436 (6.0)					800 (0.1)	1475 (0.6, br)
		−1			401 (41.4)							
OEP	OEP	0			385 (14.2)	472 (sh)		535 (0.2)	577 (0.8)	646 (w, br)		
		+1			372 (9.8)			531 (0.2)	576 (0.1)			1365 (0.5, br)
		+2			358 (8.5)			557 (0.2)			876 (1.0, br)	1380 (w, br)
		−1			387 (10.0)	401 (sh)		537 (0.1)	577 (0.1)		822 (0.2)	
TPP	OEP	0			395 (37.3)	486 (1.3)		544 (1.4)	584 (0.6)	632 (0.4)		
		+1			370 (15.6)			555 (0.9)	610 (0.7)			1300 (0.6, br)
		+2			365 (15.6)			555 (0.7)	595 (sh)		975 (0.2, br)	1300 (0.3, br)
		−1			396 (35.5)	484 (1.3)		545 (1.2)	587 (0.6)	638 (sh)		

[a] In pyridine. sh = shoulder; w = weak; br = broad.

approach of the two macrocycles to each other and may influence the potentials for both oxidation and reduction.

The cyclic voltammograms are well-defined in both CH_2Cl_2 and toluene/CH_3CN, and examples of current–voltage curves in the latter mixed solvent system are shown in Figure 5 for the case of Th(OEP)$_2$, Th(OEP)(TPP), and Th(OEP)(Pc). Each electrode process, except for those located at the positive or negative potential limits of the solvent, is characterized by a peak-to-peak separation, $|E_{pa} - E_{pc}|$, of 60 ± 5 mV and a constant value of $i_p/\nu^{1/2}$. These data suggest diffusion-controlled one-electron transfers, and this is confirmed by controlled potential coulometry which gives values of $n = 1.0 \pm 0.1$ when electrolysis is carried out at potentials positive of the first and second one-electron oxidations. On the other hand, very high n values are obtained for bulk electrolysis at potentials cathodic of the first reduction, and this suggests a demetalation of the complex on the longer time scale of bulk electrolysis.

Values of $E_{1/2}$ for processes close to the solvent limit can sometimes be obtained at high potential scan rate or alternatively by differential pulse voltammetry. Examples of data obtained with this latter technique are illustrated in Figure 6 for the case of U(OEP)$_2$, U(OEP)(TPP), and U(OEP)(Pc), two of which show a fourth reduction. Unfortunately, the products of electrode reductions at very negative potentials could not be spectrally characterized due to their proximity to the solvent edge, and it was therefore not possible to ascertain if these oxidations or reductions might be associated with one or more decomposition products.

Neutral and singly-oxidized M(OEP)(TPP) derivatives have been characterized as having a single mixed orbital involving both macrocycles,[14,19-22] and the electrochemistry of M(OEP)(TPP) also indicates this to be the case. The HOMO-LUMO gap, as expressed by $E_{1/2}(ox) - E_{1/2}(red)$, increases from 1.78 V for U(OEP)$_2$ to 1.88 V for U(OEP)(TPP) and finally to 1.98 V for U(TPP)$_2$ in CH_2Cl_2 (see Figure 7). A similar shift in the HOMO-LUMO gap is seen for the three Th(IV) bis-porphyrin derivatives which show a $\Delta E_{1/2}$ of 1.85 V for Th(OEP)$_2$, 1.95 V for Th(OEP)(TPP), and 2.06 V for Th(TPP)$_2$. The HOMO-LUMO gaps of Th(OEP)(TPP) and U(OEP)(TPP) are the exact average of those for the homoleptic M(OEP)$_2$ and M(TPP)$_2$ compounds (M = Th or U), and this provides further evidence for the occurrence of a single mixed orbital involving both macrocycles.

As previously discussed, the UV–visible data also show a systematic shift of the Soret band maximum upon going from M(OEP)$_2$ to M(OEP)(TPP) and finally to M(TPP)$_2$. The values of λ_{max} also linearly correlate with both the first oxidation and the first reduction potential of the three bis-porphyrin complexes. Thus, as expected, both the spectroscopic and electrochemical properties of M(OEP)(TPP) are exactly midway between those of M(OEP)$_2$ and M(TPP)$_2$, consistent with a single orbital involving the two macrocycles.

Similar conclusions are obtained when comparing $E_{1/2}$ values for either the first oxidation or the first reduction of M(OEP)(TPP), M(OEP)$_2$, and M(TPP)$_2$. For example, Th(OEP)(TPP) is reduced at −1.40 V and oxidized at 0.55 V and each half-wave potential lies exactly midway between the $E_{1/2}$ for reduction or oxidation of Th(TPP)$_2$ and Th(OEP)$_2$ (see Figure 8). In contrast, the half-wave potential for the second oxidation of Th(OEP)(TPP) (1.05 V) is closer to $E_{1/2}$ for the second oxidation of Th(TPP)$_2$ (1.13 V) than to Th(OEP)$_2$ (0.85 V). This result is consistent with the suggestion that the hole of [M(OEP)(TPP)]$^+$ is more localized on the OEP site than on the TPP one.[14,19-22] As such, one might expect the second oxidation to occur more at TPP than at OEP in the ultimate formation of [M(OEP$^{+\bullet}$)(TPP$^{+\bullet}$)]$^{2+}$ from [M(OEP$^{+\bullet}$)(TPP)]$^+$.

An opposite trend is obtained when comparing reduction potentials of M(OEP)(Pc) to those of M(OEP)$_2$ and M(Pc)$_2$. For example, the first reduction of Th(OEP)(Pc) is closer to $E_{1/2}$ for reduction of Th(Pc)$_2$ than to $E_{1/2}$ for reduction of Th(OEP)$_2$ (see Figure 8). This indicates a larger substituent effect of the Pc group on the site of electron transfer and strongly suggests

Table VI. UV–Visible Spectral Data of Neutral and Electrogenerated Uranium Double-Decker Complexes in CH_2Cl_2 Containing 0.2 M TBA(ClO_4)

macrocycles		charge	λ, nm (10^{-4} ε, dm^3 mol^{-1} cm^{-1})								
			Pc	Soret	Q″	Q′				NIR	
Pc	Pc[a]	0	339 (6.9)			593 (sh)	644 (9.0)	701 (2.1)			
		+1	337 (6.6)			593 (sh)	644 (6.0)	696 (3.3)			
		−1	339 (6.1)			594 (5.6)	642 (3.7)		794 (1.4)		
		−2	336 (4.7)			561 (4.8)	595 (sh)		867 (0.3)		
Pc	TPP	0	335 (8.5)	412 (10.3)	481 (3.7)	583 (1.6)	636 (2.3)	745 (sh)	829 (1.4)		
		+1	334 (4.6)	402 (4.7)	476 (1.9)	590 (sh)	636 (0.7)	738 (0.1)	846 (0.2)	1040 (0.3)	1270 (0.2, br)
		+2	325 (sh)	388 (5.1)	498 (1.6)			700 (sh)		1075 (0.6, br)	
		−1	334 (4.1)	415 (8.1)	495 (3.0)	537 (2.8)	595 (sh)	632 (3.7)			
		−2	332 (3.8)	425 (12.1)		530 (sh)	606 (3.9)		850 (br)		
Pc	OEP	0	340 (10.1)	395 (6.8)	466 (2.6)		620 (3.3)		870 (0.8)		
		+1	340 (9.4)	393 (6.1)	466 (2.3)		622 (2.1)		877 (w, br)	1170 (0.7, br)	1440 (0.9, br)
		+2	340 (8.9)	393 (5.0)	471 (2.4)		629 (0.5)		950 (0.4, br)		1350 (0.1, br)
		−1	338 (7.9)	395 (7.1)	466 (2.5)		620 (3.5)		870 (1.0)		
		−2	334 (4.6)	406 (6.9)	466 (2.8)		620 (3.2)				
					492 (2.5)						
Pc	TpTP	0	337 (8.6)	414 (11.0)	482 (4.2)	588 (1.9)	631 (2.3)	740 (sh)	825 (1.5)		
		+1	335 (6.5)	410 (7.0)	482 (3.0)	590 (sh)		727 (w)			
		+2	330 (4.6)	389 (5.7)	496 (1.8)			700 (sh)			
		−1	335 (4.6)	415 (10.2)	495 (2.6)	536 (2.3)	590 (sh)	627 (2.5)			
		−2	330 (2.8)	425 (9.4)		516 (3.0)	544 (2.9)	602 (2.5)	810 (br)		
TPP	TPP	0		407 (28.0)	487 (2.3)	553 (1.5)	622 (0.7)				
		+1		406 (19.9)		550 (sh)					1250 (0.4, br)
		+2		388 (15.6)		560 (sh)				1000 (0.8, br)	1250 (0.5, br)
		−1		417 (19.6)				730 (0.6)	848 (0.4)		
		−2		421 (14.8)			630 (sh)		800 (0.6)		
OEP	OEP	0		386 (16.6)	477 (sh)	540 (0.9)	582 (1.9)	660 (w, br)			
		+1		372 (12.6)		532 (0.8)	581 (0.4)			1170 (0.5, br)	1270 (0.6, br)
		+2		357 (11.8)		546 (0.9)			811 (1.1, br)		1250 (0.1, br)
		−1		390 (13.0)		585 (1.0)			805 (0.3)		
TPP	OEP	0		397 (19.4)	492 (0.9)	550 (1.0)	588 (sh)	655 (w, br)			
		+1		372 (10.9)		550 (0.7)				1190 (0.6, br)	
		+2		370 (10.8)	440 (sh)	570 (0.8)			885 (0.9, br)		
		−1		399 (15.2)		545 (sh)	588 (sh)	745 (0.2)	848 (0.1)		

[a] In pyridine. sh = shoulder; w = weak; br = broad.

that the first added electron is localized more on a phthalocyanine orbital type than on a porphyrin one. In contrast, the second and third reductions of Th(OEP)(Pc) occur at potentials just in between $E_{1/2}$ values for the reduction of $Th(Pc)_2$ and $Th(OEP)_2$. This suggests that there is an evenly distributed substituent effect of both macrocyclic ligands on the site of the second and third electron transfers which involve both the OEP and Pc ligands.

UV–Visible Spectra of Electrooxidized and Electroreduced Complexes. The 14 investigated compounds were stepwise oxidized or reduced in a thin-layer cell as the *in situ* UV–visible spectra were measured as a function of time. Examples of the resulting spectra taken during the first two oxidations and first two reductions of representative U and Th derivatives containing one porphyrin and one phthalocyanine macrocycle are shown in Figure 9. Isobestic points are obtained during each electron transfer, and this demonstrates the lack of spectral intermediates on the thin-layer spectroelectrochemical time scale. A summary of the spectroscopic data for all of the neutral, electrooxidized, and electroreduced complexes is given in Tables V and VI, while Figure 10 illustrates representative UV–visible spectra of $[M(P)(Pc)]^n$ where M = Th or U, P = OEP or TpTP, and n = 0, 1+, or 2+.

The UV–visible spectra for compounds in a given $[M(P)_2]^n$, $[M(P)(Pc)]^n$, or $[M(P)(P')]^n$ series will depend upon both the type of metal ion (Th or U) and the overall charge of the complex. As earlier discussed, neutral M(P)(Pc) has two major bands. The first is located at 335–340 nm and is associated with the presence of a phthalocyanine macrocycle in the complex. The second is assigned to the porphyrin macrocycle and occurs at 412–413 (TPP) or 393–395 nm (OEP).

The intensity of the porphyrin band of M(P)(Pc) decreases relative to that of the Pc band upon the first two electrooxidations. This is shown in Figure 10 for the case of U(OEP)(Pc) and Th(TpTP)(Pc) and implies that the site of electrooxidation involves more the porphyrin than the Pc ring. Only small changes occur in the Pc band upon the first oxidation of U(OEP)(Pc) (Figure 9), but much larger changes are seen upon formation of $[Th(TpTP)(Pc)]^+$ or $[Th(TpTP)(Pc)]^{2+}$. These data are self-consistent and imply a greater charge density on $[Th(TpTP)(Pc)]^+$ than on $[U(OEP)(Pc)]^+$.

Figure 9 also illustrates the changes that occur upon the stepwise reduction of M(P)(Pc) to $[M(P)(Pc)]^-$ to $[M(P)(Pc)]^{2-}$. The Pc band decreases substantially in intensity during addition of the first electron which thus implies that Pc is preferentially reduced. This is also the conclusion from comparisons of redox potentials in Figure 8. The Soret band is unaffected by the addition of one electron to U(OEP)(Pc) but decreases slightly in intensity upon the first reduction of Th(TpTP)(Pc). A further decrease in the Pc band intensity is seen upon conversion of $[M(P)(Pc)]^-$ to $[M(P)(Pc)]^{2-}$, and this change is accompanied by a red shift of the porphyrin Soret band. This implies further reduction at the Pc macrocycle but is also consistent with an orbital having some OEP or TpTP anion radical character. Again, similar conclusions can be reached by analysis of the electrochemical data for U(P)(Pc) or Th(P)(Pc), the latter of which is shown in Figure 8.

Relative ratios of molar absorptivities between the Pc and P bands of $[M(P)(Pc)]^n$ where $n \approx 0$, 1±, or 2± are listed in Table VII as a function of the porphyrin ring (OEP, TPP, or TpTP) and complex oxidation state. The trends in the spectral changes are similar upon oxidation or reduction of $[Th(P)(Pc)]^n$ and $[U(P)(Pc)]^n$ (see Figures 9 and 10), but the ratio of the porphyrin to phthalocyanine molar absorptivity is in all cases higher for the Th(IV) than for the U(IV) derivatives. The data thus show that the UV–visible spectra depend upon the specific actinide metal ion and are not interchangeable for U and Th complexes having

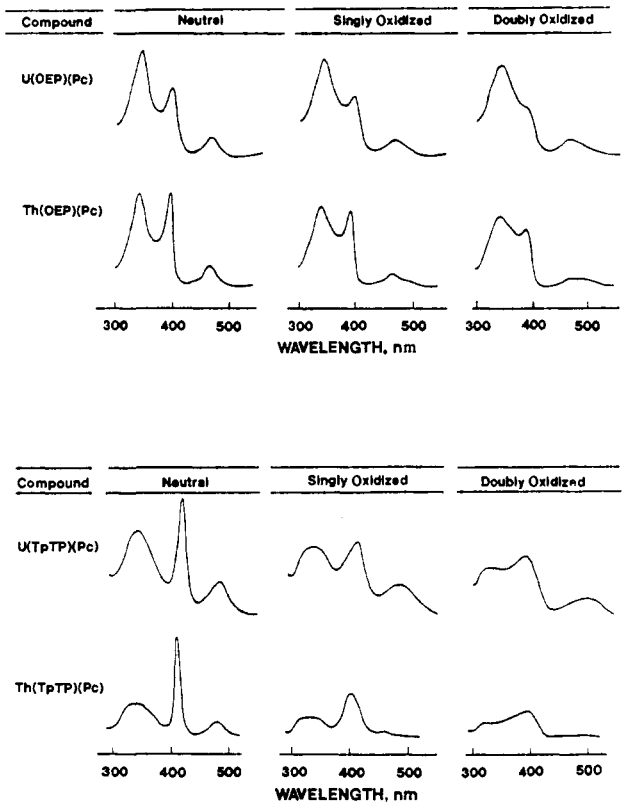

Figure 10. UV–visible spectra of $[M(P)(Pc)]^n$ in CH_2Cl_2 containing 0.2 M $TBA(ClO_4)$ where M = Th or U, n = 0, 1+, or 2+, and P = OEP or TpTP.

Table VII. Ratio of Molar Absorptivities between the Pc Band (λ_{max} = 320–341 nm) and the Porphyrin Band (λ_{max} = 388–425 nm) of $[M(P)(Pc)]^n$ (n = 0, 1±, or 2±) in CH_2Cl_2 Containing 0.2 M $TBA(ClO_4)$

oxidation state, n	porphyrin macrocycle, P	ϵ_{Pc}/ϵ_P ratio	
		$[U(P)(Pc)]^n$	$[Th(P)(Pc)]^n$
0	OEP	1.49	1.02
	TPP	0.83	0.41
	TpTP	0.78	0.42
+1	OEP	1.54	1.06
	TPP	0.98	0.50
	TpTP	0.93	0.44
+2	OEP	1.78	1.24
	TPP	*a*	*a*
	TpTP	0.81	0.51
−1	OEP	1.11	0.83
	TPP	0.51	0.15[b]
	TpTP	0.45	0.25[b]
−2	OEP	0.67	0.78
	TPP	0.31	0.20
	TpTP	0.30	0.20

[a] Maxima of Pc bands could not be determined due to broadness of absorption. [b] Large uncertainty due to peak broadening.

the same oxidation state and the same set of porphyrin and/or phthalocyanine macrocycles.

FTIR Spectra of Chemically and Electrochemically Oxidized Compounds. Figure 11 illustrates thin-layer FTIR spectra obtained after the first two electrooxidations of $U(OEP)_2$ in CH_2Cl_2. Singly-oxidized $[U(OEP)_2]^+$ exhibits a strong infrared band at 1526 cm^{-1} (solid line in Figure 11) consistent with formation of a porphyin π-cation radical.[33] This band is blue shifted by 19 cm^{-1} and increases in intensity upon abstraction of a second electron to give the doubly-oxidized species which can be formally considered as containing two porphyrin π-cation radicals, i.e. $[U(OEP^{\bullet+})(OEP^{\bullet+})]^{2+}$. Similar infrared marker bands are seen for the $SbCl_6^-$ porphyrin derivatives in the solid state, and examples of the resulting spectra are shown in Figure 12 for $[U(OEP)_2]^+$,

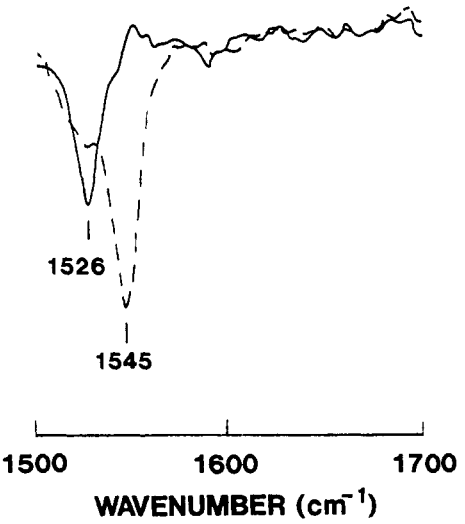

Figure 11. FTIR spectra showing the diagnostic π-cation radical marker band of electrogenerated $[U(OEP)_2]^+$ (—) and $[U(OEP)_2]^{2+}$ (- - -) in CH_2Cl_2 containing 0.2 M $TBA(ClO_4)$.

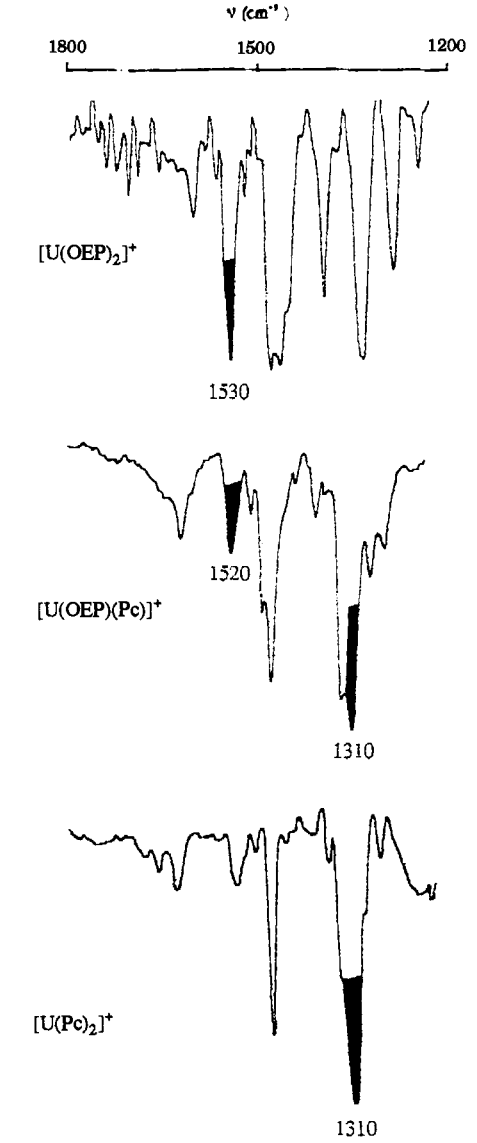

Figure 12. Solid-state IR spectra of $[U(OEP)_2]^+SbCl_6^-$, $[U(OEP)(Pc)]^+SbCl_6^-$, and $[U(Pc)_2]^+SbCl_6^-$.

$[U(OEP)(Pc)]^+$, and $[U(Pc)_2]^+$. The relevant IR bands for these and the other complexes are summarized in Table VIII.

Table VIII. Diagnostic Infrared π-Cation Radical Marker Bands (cm^{-1}) of Singly- and Doubly-Oxidized Complexes in CH_2Cl_2 Containing 0.1 M TBA(ClO_4)

			singly oxidized			
			Pc band	porphyrin band		doubly oxidized[b]
metal	macrocycles		solid[a]	solid[a]	solution[b]	porphyrin band
U	OEP	Pc	1310	1520	1510	1525
		OEP		1530	1526	1545
		TPP		1534	1574, 1522	1525
	TPP	Pc	1310	1260		
		OEP		1262		
		TPP		1266		
	Pc	Pc	1310			
Th	OEP	Pc	1310	1515	1510	1518
		OEP		1521	1518	1536
		TPP		1525	1570, 1522	1516
	TPP	Pc	1310	1267		
		OEP		1270		
		TPP		1263		
	Pc	Pc	1306			

[a] Values obtained for chemically generated $SbCl_6^-$ salt in CsI. [b] Electrogenerated species in CH_2Cl_2 containing 0.1 M TBA(ClO_4).

Octaethylporphyrin π-cation radical marker bands of the chemically generated $SbCl_6^-$ derivatives are seen between 1515 and 1534 cm^{-1} in the solid state, and this is consistent with data in the literature for other singly-oxidized double-decker species containing an OEP macrocycle.[2,3,14,17] For example, this band appears at 1530 and 1520 cm^{-1} for chemically generated $[U(OEP)_2]^+$ and $[U(OEP)(Pc)]^+$, respectively. These marker bands are also seen at 1510 and 1526 cm^{-1} in solution for the electrooxidized species having either one or two OEP rings and, as might be expected, these values shift to 1518 and 1545 cm^{-1}, respectively, after abstraction of a second electron from the complex to give the doubly-oxidized species. The intensity of the band for doubly-oxidized $[U(OEP)_2]^{2+}$ is almost twice as large as that for singly-oxidized $[U(OEP)_2]^+$, suggesting that one electron has been removed from each of the two porphyrin rings, each of which behaves as an independent π-cation radical in terms of the IR marker bands. Likewise, the IR spectra of $[M(OEP)(TPP)]^{2+}$ and $[M(OEP)(Pc)]^{2+}$ can both be interpreted in terms of bis-π-cation radicals of the type $[M(OEP^{\bullet+})(TPP^{\bullet+})]^{2+}$ and $[M(OEP^{\bullet+})(Pc^{\bullet+})]^{2+}$.

Unfortunately, no TPP π-cation radical marker bands could be experimentally observed for the electrooxidized complexes, and this was due in large part to the fact that these bands would be overlapped with bands of the TBA(ClO_4) supporting electrolyte.[31] However, π-cation radical marker bands of TPP are clearly evident in the chemically generated $SbCl_6^-$ species. For example, $[M(TPP)_2]^+$ has a band at 1263 cm^{-1} (M = Th) or 1266 cm^{-1} (M = U) while $[M(TPP)(Pc)]^+$ has a band at 1267 cm^{-1} (M = Th) or 1260 cm^{-1} (M = U). The $[U(Pc)_2]^+$ species shows an extra band at 1310 cm^{-1} which is also observed for singly-oxidized $[U(OEP)(Pc)]^+$ (see Figure 12). To our knowledge, this band has never been reported as a marker band for oxidized phthalocyanine complexes, but it is clearly present in all of the investigated singly-oxidized $[M(P)(Pc)]^+$ species. In this regard, it should be pointed out that the phthalocyanine marker band is also accompanied by an OEP or TPP π-cation radical band in singly oxidized $[(M)(P)(Pc)]^+$, and this further suggests a delocalization of the single positive charge over both the porphyrin and the phthalocyanine macrocycles. The same result is also seen for $[M(OEP)(TPP)]^+$ which shows both OEP^+ and TPP^+ marker bands (see Table VIII), again demonstrating the mixed orbital character of the singly oxidized heteroleptic compounds.

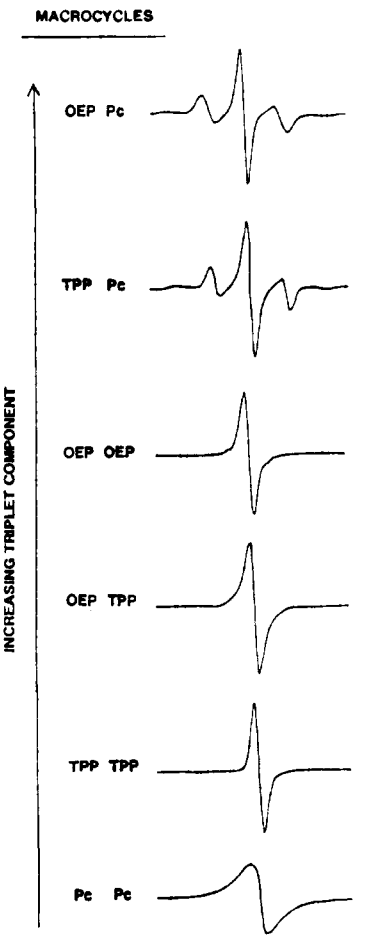

Figure 13. ESR spectra illustrating the presence or absence of the triplet component in frozen CH_2Cl_2 solutions containing 0.1 M TBA(ClO_4) at 110 K.

ESR of Singly-Oxidized Th Compounds. The neutral double-decker complexes were chemically converted to their singly-oxidized forms as described in the Experimental Section and their ESR spectra were then recorded for the chemically-generated $SbCl_6^-$ salt both as a solid and in frozen solution. Each solid singly-oxidized species has a signal centered at $g = 2.003$ and a peak-to-peak separation, ΔH, of 1.7 to 5.8 G (see Table IX). Slightly higher values of ΔH are obtained for the symmetrical $[Th(TPP)_2]^+$ (5.1 G) and $[Th(OEP)_2]^+$ (5.8 G) complexes while lower values are seen for $[Th(Pc)_2]^+$ and the nonsymmetrical $[Th(OEP)(TPP)]^+$ (2.9 G) or $[Th(P)(Pc)]^+$ (1.7–2.0 G) derivatives.

Table IX. ESR Properties for Chemically Oxidized Double-Decker Thorium Complexes at 110 K[a]

		solid state		in CH_2Cl_2		in CH_2Cl_2, 0.1 M TBA(ClO_4)		in pyridine	
macrocycles		g	ΔH, G	g	ΔH, G	g	ΔH, G	g	ΔH, G
OEP	Pc	2.003	2.0	2.003	3.9	2.003	3.5	2.003	5.4
TPP	Pc	2.003	1.7	2.003	5.4	2.003[b]	3.6	2.003	5.9
OEP	OEP	2.003	5.8	2.003	4.8	2.003	4.3	2.003	1.8
OEP	TPP	2.003	2.9	2.002	8.1	2.003	4.7	2.003	5.4
TPP	TPP	2.002	5.1	2.001	4.8	2.001	5.0	2.001	6.4
Pc	Pc	2.003	2.0	2.003	3.0	2.003	8.3	2.003	3.5

[a] Species added to solution as $SbCl_6^-$ salt. [b] Electrochemically generated cation.

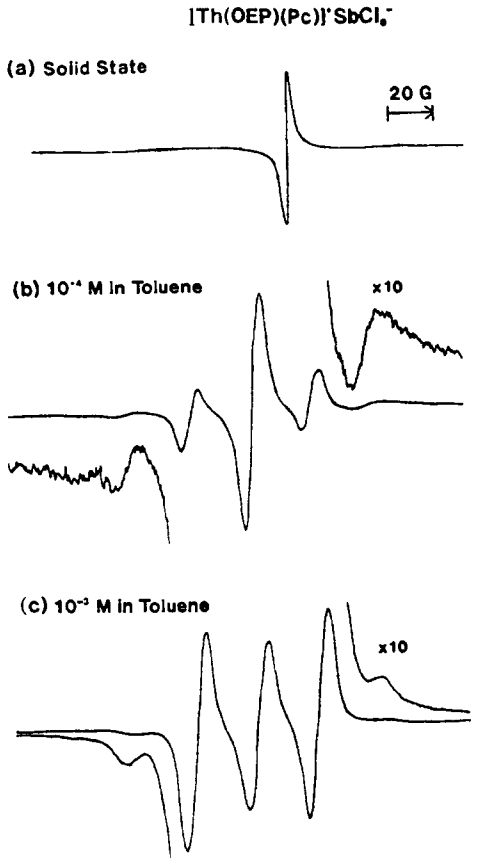

Figure 14. ESR spectrum of $[Th(OEP)(Pc)]^+$ at 110 K (a) as a solid sample of the $SbCl_6^-$ salt, (b) in frozen toluene at a concentration of 10^{-4} M, and (c) in frozen toluene at a concentration of 10^{-3} M.

Table X. Comparison of Triplet State Parameters Observed for OEP-Pc and TPP-Pc Thorium Complexes at 110 K[a]

	in CH_2Cl_2		in CH_2Cl_2, 0.1 M $TBA(ClO_4)$		in pyridine	
macrocycle	g	D, 10^4 cm^{-1}	g	D, 10^4 cm^{-1}	g	D, 10^4 cm^{-1}
OEP-Pc	2.002	38.8	2.003	37.3	2.002	37.5
TPP-Pc	2.003	36.5	2.003[b]	35.8		

[a] Species added to solution as $SbCl_6^-$ salt. [b] Electrochemically generated cation.

On the other hand, quite different ESR data are obtained for the nonsymmetrical $[Th(OEP)(Pc)]^+$ and $[Th(TPP)(Pc)]^+$ derivatives in frozen solution at 110 K. This is illustrated in Figures 13 and 14 where the ESR spectral envelope consists of two sets of superimposed resonances. One is due to a central line similar to those discussed above while the other is due to a pair of lines which are similar to the two pairs of spectral lines expected for a randomly-oriented solid solution of a triplet state radical for which $E = 0$.[45] Table IX lists the g values and line widths for the central line in frozen solutions of (i) CH_2Cl_2, (ii) CH_2Cl_2 containing 0.1 M $TBA(ClO_4)$, and (iii) pyridine while Table X lists the D value (zero field splitting parameter in cm^{-1}) under the same experimental conditions. The data in CH_2Cl_2 are consistent with the presence of a triplet state, but attempts to observe the half-field (i.e., $g = 4$) resonance which would have confirmed this assignment were unsuccessful. However, this is not surprising because the relative intensity of the half-field resonance to that of the full-field resonance is proportional to the ratio of D (the zero field splitting parameter) to the value of the field at $g = 2$.[46,47]

(45) Wertz, J. E.; Bolton, J. R. *Electron Spin Resonance*; McGraw Hill Book Company: New York, 1972; p 238.

Scheme I

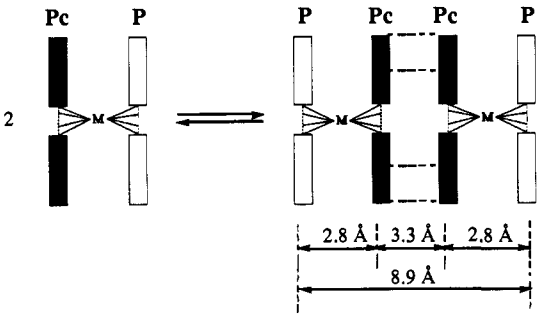

Neither $[Th(Pc)_2]^+$, $[Th(TPP)_2]^+$, nor $[Th(OEP)(TPP)]^+$ shows triplet-state character in frozen CH_2Cl_2 solution at 110 K while $[Th(OEP)_2]^+$ displays small satellite peaks under these experimental conditions. Both $[Th(OEP)(Pc)]^+$ and $[Th(TPP)(Pc)]^+$ have well-defined triplet-state character in CH_2Cl_2 (which is much decreased in pyridine), and this can be interpreted in terms of π–π interactions between two singly-oxidized $[Th(P)(Pc)]^+$ species in the low dielectric constant solvent.

ESR measurements were also made for $[Th(OEP)(Pc)]^+$ at two different concentrations in toluene. The resulting data are shown in Figure 14 which also illustrates the ESR spectrum of the same compound as a $SbCl_6^-$ salt in the solid state. $[Th(OEP)(Pc)]^+$ shows a well-defined triplet-state component in frozen solution which is not present in the solid material. The triplet component is higher at the larger investigated concentration (10^{-3} M) and this suggests the occurrence of an equilibrium between dissociated and associated porphyrin π-cation radicals of the type shown in Scheme I where M = Th and P = OEP or TPP.

The occurrence of π–π interactions between porphyrin π-cation radicals was initially shown to occur for singly-oxidized complexes of the type $[M(OEP)]^+$ (M = Mg, Zn)[48,49] and was more recently demonstrated for several singly-oxidized Zn(II) and Ni(II) derivatives which were crystallographically characterized and had a porphyrin–porphyrin distance of 3.31 and 3.19 Å, respectively.[50] Similar π–π interactions are proposed to occur for singly-oxidized $[Th(P)(Pc)]^+$ and it is suggested that these involve the Pc rather than the OEP macrocycles as shown in Scheme I.

The average (r_{av}) distance between the two unpaired electrons in singly-oxidized $[Th(OEP)(Pc)]^+$ was calculated with use of the data given in Table X and eq 4 where r_{av} is expressed in Å, g is the g value of the radical, and the zero field parameter, D, is given in cm^{-1}.[51,52]

$$r_{av} = \sqrt[3]{\frac{0.65g^2}{D}} \qquad (4)$$

The measured value of D for $[Th(P)(Pc)]^+$ varies from 35.8 to 38.8 $\times$ 10^{-4} cm^{-1}, depending upon the specific porphyrin macrocycle (TPP or OEP) and solution conditions, and this corresponds to an average distance of 8.8–9.0 Å between the two porphyrin planes of the π-cation radical. The experimental

(46) Dubois, D.; Jones, M. T.; Kadish, K. M. *J. Am. Chem. Soc.* **1992**, *114*, 6446–6451.
(47) Jones, M. T. Private communication.
(48) Felton, R. H. In *The Porphyrins*; Dolphin, D., Ed.; Academic Press: New York, 1978; Vol. V, p 81.
(49) Song, H.; Reed, C. A.; Scheidt, W. R. *J. Am. Chem. Soc.* **1989**, *111*, 6867–6868.
(50) Song, H.; Orosz, R. D.; Reed, C. A.; Scheidt, W. R. *Inorg. Chem.* **1990**, *29*, 4274–4282.
(51) Lazarev, G. G. *Z. Phys. Chem.* **1991**, *173*, 141–165.
(52) Wertz, J. E.; Bolton, J. R. *Electron Spin Resonance*; McGraw Hill Book Company: New York, 1972; p 230.

average distance of 8.9 Å between the two unpaired electrons in $[Th(P)(Pc)]_2^{2+}$ can thus be interpreted in terms of an average 3.3-Å separation between the two interactive phthalocyanine planes. Our calculated value is based on the assumption that the difference between the porphyrin and the phthalocyanine macrocycles of $[Th(P)(Pc)]^+$ is the same as that between the two macrocycles of $[Ce(TPP)(Pc)]^+$ (2.78 Å).[28] It also assumes a flattening of the Pc ring in the interacting dimer. Both assumptions are not unreasonable and lead to values which are in excellent agreement with the crystallographic separation of 3.19–3.31 Å between the two porphyrin planes of $[M(OEP)]_2^{2+}$ (M = Zn, Ni).[49,50]

In summary, our assignment of the dimer shown in Scheme I is based in part on the fact that the Pc macrocycle is more planar than OEP, in part on the spectroelectrochemical data which show the oxidation site to be more localized on OEP or TPP than on the Pc macrocycles of $[Th(P)(Pc)]^+$, and in part on a calculation of the average distance between the two unpaired electrons of the triplet. It is also in agreement with the electrochemical data which indicate that $[Th(OEP)(Pc)]^+$ has two sets of separate orbitals and a positive charge localized more on the porphyrin than on the phthalocyanine ring. However, it must be emphasized that a $\pi-\pi$ interaction does not seem to occur through the sterically hindered TPP rings of $[Th(TPP)(Pc)]^+$. The fact that a triplet is experimentally observed gives even further evidence for interactions occurring through the Pc rather than the porphyrin macrocycles of $[Th(P)(Pc)]_2^{2+}$.

Finally, it should be noted that triplet ESR spectra have been reported for the product formed after the ring centered oxidation of several dimeric cofacial porphyrins in the "Pacman" series[53,54] as well as for a neutral covalently linked dicopper diporphyrin.[55] The two electrons are abstracted from the same molecule in both sets of compounds, and the results in this present study thus present the first ESR evidence for electronic coupling between two separate porphyrin π-cation radicals in solution.

Acknowledgment. The support of the National Science Foundation (K.M.K., Grant No. CHE-8822881), the Robert A. Welch Foundation (K.M.K., Grant E-680), and C.N.R.S. is gratefully acknowledged. The authors also acknowledge helpful discussions with Professor M. Thomas Jones on the ESR sections of this manuscript.

(53) Collman, J. P.; Denisevitch, P.; Konai, Y.; Marroco, M.; Koval, C.; Anson, F. C. *J. Am. Chem. Soc.* **1980**, *102*, 6027–6036.
(54) Le Mest, Y.; L'Her, M.; Hendricks, N. H.; Kim, K.; Collman, J. P. *Inorg. Chem.* **1992**, *31*, 835–847.
(55) Eaton, S. S.; Eaton, G. R.; Chang, C. K. *J. Am. Chem. Soc.* **1985**, *107*, 3177–3184.